Title

A broad exploration of nonlinear dynamics in microbial systems motivated by chemostat experiments producing deterministic chaos.

Authors

Molz, Fred

Faybishenko, Boris

Agarwal, Deborah

Publication Date

2024-01-21

Peer reviewed

A Broad Exploration of Coupled Nonlinear Dynamics in Microbial Systems Motivated by Chemostat Experiments Producing Deterministic Chaos.

Fred Molz[1], Boris Faybishenko[2] and Deborah Agarwal[3]

[1]Environmental Engineering & Earth Sciences Dept., Clemson University, 342 Computer Court, Anderson, SC 29625.

[2]Energy Geosciences Division, Earth and Environmental Sciences Area, Lawrence Berkeley National Laboratory, Berkeley, CA 94720

[3]Computer Research Division, Lawrence Berkeley National Laboratory, Berkeley, CA 94720

LBNL Report Number LBNL-2001172

Acknowledgements BF and DA research supported by the U.S. DOE, Office of Science, Office of Biological and Environmental Research, and Office of Science, Office of Advanced Scientific Computing under the DOE Contract No. DE-AC02-05CH11231. FM acknowledges the support of the Clemson University, Department of Environmental Engineering and Earth Sciences.

Table of Contents.

ABSTRACT.

The main objective of this report is to develop an exploratory mathematical analysis motivated by the Becks et al. (2005) experiments, which will be presented in Chapter 1. Related details of the resulting model will be presented in Chapter 2, and a detailed non-dimensionalization will follow in Chapter 3. During the research to be described, a potential relationship to Shannon information theory was realized, and this will be developed in Chapter 4. Several avenues for future research are suggested, and a more mathematically-oriented presentation of the non-linear dynamical properties of the equations developed in Chapter 1 may be found in Faybishenko et al. (2018).

Chapter 1: Mathematical Analysis of the Becks et al. (1995) Experiments.

1.1. Introduction.

Deterministic chaotic dynamics in biological systems has not received as much attention as that in electronic or fluid-mechanical systems, and mathematical models are at an early stage of development (Faybishenko and Molz (2013). However, this has started to change. Molz and Faybishenko (2013) have recently concluded that three papers (Becks et al, 2005; Graham et al. 2007; Beninca et al., 2008), using experimental studies and relevant mathematics, may provide convincing demonstrations that deterministic chaos is present in relatively simple biochemical systems of an ecological nature. (See Constantino et al., 1997 for additional support.) For example, Graham et al. (2007) reported experimental results demonstrating the phenomenon of chaotic instability in biological nitrification in a controlled laboratory environment. In this study, the aerobic bioreactors (aerated containers of nutrient solution and microbes) were filled initially with a mixture of wastewater from a treatment plant and simulated wastewater involving a mixture of many microbes. The main variables recorded as a time series were total bacteria, ammonia-oxidizing bacteria (AOB), nitrite-oxidizing bacteria (NOB), and protozoa, along with effluent concentrations of nitrate, nitrite and total ammonia. The method of Rosenstein et al. (1993) was used to calculate Lyapunov exponents, which fell roughly in a range from 0.05 to 0.2 d^{-1}. Graham et al. (2007) concluded that "nitrification is prone to chaotic behavior because of a fragile AOB-NOB mutualism," i.e., interaction.

Beninca et al. (2008) conducted a laboratory experiment over a period

of 6.3 years, which demonstrated chaotic dynamics in a plankton community in a water sample obtained from the Baltic Sea. This experiment was housed in a cylindrical container that was 45 cm in diameter, 74 cm high and filled with 90 l of water with a 10 cm sediment layer at the bottom. The "predictability" of each data set was shown to decrease with time (essentially lost after 15 - 30 days), consistent with positive Lyapunov exponents averaging about 0.058 per day. While small, these numbers are significantly above zero because of the large amount of data collected. They were calculated based on 2 methods: attractor reconstruction using time-delay plots, and direct calculation of the Lyapunov exponents (Kantz and Schreiber, 1997). It is apparent that when dealing with exponential divergence of trajectories in phase-space, the dominant and positive Lyapunov exponent does not have to be large for the phenomenon of chaotic dynamics to be important.

A particularly detailed experiment was that of Becks et al. (2005). That team studied a microbial food web in a chemostat, with additional analyses presented during following years (Becks and Arndt, 2008, 2009). A conceptual model of these experiments is shown in Figure 1.1. The food web was composed of a nutrient source, 2 bacteria that consumed nutrient (a rod and a coccus), and a ciliate predator that consumed both bacteria. The variable supporting the system was the food supply that was varied by changing the

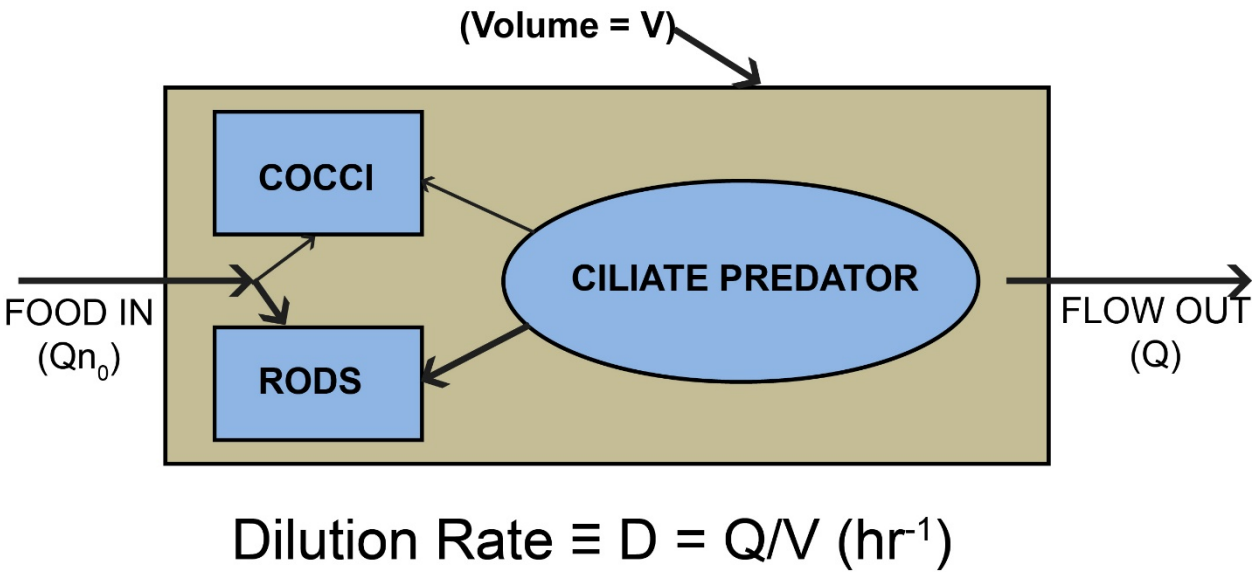

Figure 1.1. Diagram of the Becks et al. (2005) chemostat system. A nutrient solution flowing left to right was consumed by two microbes (rods and cocci), with rods being stronger competitors for nutrient than cocci. A ciliate predator fed on both microbes, but preferred rods over cocci.

dilution rate (chemostat flow through/chemostat volume, having units of inverse time). The 4 coupled dependent variables were concentrations of nutrient (mg/cc) and each of the 3 microbes (cells/cc). For a fixed set of dilution rates, the 3 microbe concentrations were measured at a selected set of approximately daily time intervals. Each set of data constituted a time series (concentrations at discrete times), and deterministic chaos was identified by using a computerized version of the analytical procedure developed by Rosenstein et al. (1993) for calculating the largest Lyapunov exponent (TISEAN package [Hegger et al., (1999)). Classical steady states were observed at D =0.9/day and 0.75/day, chaotic dynamics were observed at D = 0.5/day, and periodic dynamics were observed at a slightly lower D = 0.45/day. (See Becks et al. (2005) for additional details.)

1.2. Mathematical Model Development.

To describe the processes of the Becks et al. experiment, we first modified the original 3-equation mathematical model (nutrient plus 2 microbes) developed by Kot et al. (1992) to a 4 equation model. Four dependent variables were identified: n(t), r(t), c(t) and p(t). The units of the nutrient concentration were mg/cc, while those of the microbes were cell numbers/cc (cells/cc). Thus in order to conserve mass in the resulting model, an average microbial mass had to be selected for each microbe type. This was done based on measured microbe volume averages published by Becks et al. (2005), along with an assumed density of 1 g/cc: (r mass (m_r) = 1.6E-9 mg; c mass (m_c) = 8.2E-9 mg, and p mass (m_p) = 3.2E-6 mg). With these minor differences, the Kot et al. (1992) equations for a nutrient (mg/cc), a rod (cells/cc) and a predator (cells/cc) would be written as:

$$\frac{dn}{dt} = Dn_0 - \frac{\mu_{rn}}{Y_{rn}}\left[\frac{n(rm_r)}{K_{rn}+n}\right] - Dn \qquad (a)$$

$$\frac{d(rm_r)}{dt} = \mu_{rn}\left[\frac{n(rm_r)}{K_{rn}+n}\right] - \frac{\mu_{pr}}{Y_{pr}}\left[\frac{(rm_r)(pm_p)}{K_{pr}+(rm_r)}\right] - D(rm_r) \qquad (b) \qquad (1.1)$$

$$\frac{d(pm_p)}{dt} = \mu_{pr}\left[\frac{(rm_r)(pm_p)}{K_{pr}+(rm_r)}\right] - D(pm_p) \qquad (c)$$

These three equations are identical to those used by Kot et al. (1992), with $S = n$, $H = rm_r$, and $P = pm_p$. All the "m_x" terms are mean mass per respective microbe, so r and p are dimensionless numbers of rods and predators per cc, the microbe "concentration" units recorded by Becks et al. (2005). All the other constant terms are various maximum specific growth rates "μ_x", half

saturation constants "K_x" and yield coefficients "Y_x". (For a quick overview of Monod kinetics, see (https://en.wikipedia/wiki/Monod_equation).

To extend Equations (1.1) to include one more nutrient-consuming microbe, a cocci, an equation similar to (1.1b) is added, along with the analogous coupling terms, resulting in the following system of 4 ordinary differential equations (New terms in red.).

$$\begin{aligned}
\frac{dn}{dt} &= Dn_0 - \frac{\mu_{rn}}{Y_{rn}}\left[\frac{n(rm_r)}{K_{rn}+n}\right] - \frac{\mu_{cn}}{Y_{cn}}\left[\frac{n(cm_c)}{K_{cn}+n}\right] - Dn \\
\frac{d(rm_r)}{dt} &= \mu_{rn}\left[\frac{n(rm_r)}{K_{rn}+n}\right] - \frac{\mu_{pr}}{Y_{pr}}\left[\frac{(rm_r)(pm_p)}{K_{pr}+(rm_r)}\right] - D(rm_r) \\
\frac{d(cm_c)}{dt} &= \mu_{cn}\left[\frac{n(cm_c)}{K_{cn}+n}\right] - \frac{\mu_{pc}}{Y_{pc}}\left[\frac{(cm_c)(pm_p)}{K_{pc}+(cm_c)}\right] - D(cm_c) \\
\frac{d(pm_p)}{dt} &= \mu_{pr}\left[\frac{(rm_r)(pm_p)}{K_{pr}+(rm_r)}\right] + \mu_{pc}\left[\frac{(cm_c)(pm_p)}{K_{pc}+(cm_c)}\right] - D(pm_p)
\end{aligned} \qquad (1.2)$$

The parameters involved are once again maximum specific growth rates (μ_{xx}), half saturation constants (K_{xx}) and yield coefficients (Y_{xx}), a total of twelve. Equations (1.2) are direct generalizations of the Kot et al. (1992) model, and their mathematical validity was checked by showing that a mass balance was maintained, and when the Kot et al. (1992) initial conditions and parameter values were used, with one microbe forced to die out, output equivalent to Figure 3 of Kot et al. (1992) was reproduced. As written, however, Equations (1.2) do not include information from the supplemental experiments of Becks et al. (2005) or particular information on how a chemostat operates, such as potential nutrient recycling from dying biomass. Using Equations (1.2) alone, we were not able to produce chaotic dynamics, and it was difficult to produce solutions wherein all microbes survived indefinitely. Further details concerning the initial studies of Equations (1.2) are given in Chapter 2.

In expanding (1.2) as motivated by the Becks et al. supplemental experiments, the specific death rate of predators and their biomass recycling to nutrient are likely to be important, because their average mass is about 1000 times greater than that of each feeding microbe. Moreover, populations of feeding microbes decrease mainly due to consumption by predators, while nothing consumes the dying predators. When predators die, their bodies simply break down with remains consumed or flushed out of the well-mixed chemostat. Because of these considerations, natural death and biomass recycling of the feeding microbes is assumed to be negligible relative to predators, and this was supported also by numerical experiments. The specific death rate for predators and the nutrient recycling terms will be identified in the final equation set that is developed.

As observed in the Becks et al. supplemental experiments, in the absence of predators r was able to out-compete c for nutrient, and at an identical population of r and c ($4x10^6$ cells/cc), p consumed r cells over c cells in the ratio of 4:1. In the absence of further guidance from the experiments, we decided to incorporate the additional information into Equations (1.2), to arrive at Equations (1.10), as follows: 1) When *r* and *c* are low, *p* chooses them on an equal basis even though in general *r* is preferred over *c* (Starving organisms are not choosy?), 2) At high *r* and *c*, as observed in the experiments, p chooses *r* four times more than *c,* and 3) in competition for nutrient with no predators, the cocci will die out first.

A simple way to impose condition 3, is to set the value of μ_{rn}, the maximum specific growth rate of r on n, equal to $k\mu_{cn}$, with $k > 1$. Then for k sufficiently large, r will always outcompete c. Incorporating conditions 1 and 2 is more involved, but it is still straightforward.

Based on the Becks et al. [1995, Figure.1] data, the *r* and *c* concentrations are ranging from about $1x10^5$ cells/cc to $2x10^6$ cells/cc. On a cell numbers basis (see the 2nd and 3rd members of Equations (1.2)), the respective uptake rates of *p* on *r* (dr_p/dt) and *p* on *c* (dc_p/dt) may be expressed as:

$$\frac{dr_p}{dt} = \frac{pm_p\mu_{pr}r}{Y_{pr}(K_{pr}+m_r r)} \quad and \quad \frac{dc_p}{dt} = \frac{pm_p\mu_{pc}c}{Y_{pc}(K_{pc}+m_c c)} \tag{1.3}$$

Assuming that for the minimum values of *r* and *c* (*r* = *c* = $1x10^5$ cells/cc) $\frac{dr_p}{dt} = \frac{dc_p}{dt}$, we obtain from (1.3):

$$\frac{pm_p\mu_{pr}(1x10^5)}{Y_{pr}(K_{pr}+1x10^5 m_r)} = \frac{pm_p\mu_{pc}(1x10^5)}{Y_{pc}(K_{pc}+1x10^5 m_c)} \tag{1.4}$$

Assuming that for maximum values of *r* and *c* (*r* = *c* = $2x10^6$ cells/cc)

$$\frac{dr_p}{dt} = 4\frac{dc_p}{dt}$$

we obtain:

$$\frac{pm_p\mu_{pr}\left(2x10^6\right)}{Y_{pr}\left(K_{pr}+2x10^6 m_r\right)} = \frac{4pm_p\mu_{pc}\left(2x10^6\right)}{Y_{pc}\left(K_{pc}+2x10^6 m_c\right)} \tag{1.5}$$

We will modify the numerator and denominator of dr_p/dt, given in (1.3), in order to achieve the equalities specified in Equations (1.4) and (1.5). The maximum specific growth rate of *p* on *r* will become $\mu_{pr}(m_1 r+i_1)$, and the

denominator will become $K_{pr}+m_2r+m_rr$, with m_1, i_1 and m_2 constants. Substituting this in dr_p/dt yields

$$\frac{dr_p}{dt} = \frac{pm_p\mu_{pr}(m_1r+i_1)r}{Y_{pr}(K_{pr}+m_2r+m_rr)} \tag{1.6}$$

Thus we are making μ_{pr} and K_{pr} linear functions of r. To keep the overall units consistent, m_1 has the units of $(cells/cc)^{-1}$, i_1 is dimensionless, and m_2 has the units of mg. Eq. (1.6) is a new semi-empirical relationship expressing a modified form of the Monod kinetics equation, motivated by experiment, and is given to take into account a *p* preference change for *r* relative to c. Then to satisfy Equations (1.4) and (1.5), the following conditions must be met:

$$\begin{aligned} \frac{\mu_{pr}(10^5 m_1+i_1)}{Y_{pr}(K_{pr}+10^5 m_2+10^5 m_r)} &= \frac{\mu_{pc}}{Y_{pc}(K_{pc}+10^5 m_c)}, \quad and \\ \frac{\mu_{pr}(2x10^6 m_1+i_1)}{Y_{pr}(K_{pr}+2x10^6 m_2+2x10^6 m_r)} &= \frac{4\mu_{pc}}{Y_{pc}(K_{pc}+2x10^6 m_c)} \end{aligned} \tag{1.7}$$

The introduced parameters m_1 and i_1 must satisfy the following conditions: $10^5 m_1 + i_1 = 1$, and $2x10^6 m_1 + i_1 = 4$, also setting $\mu_{pr} = \mu_{pc}$. These conditions yield $m_1 = 1.579x10^{-6}$ *(cells/cc)*$^{-1}$ and $i_1 = 0.8421$. The corresponding conditions on m_2 are:

$$\begin{aligned} Y_{pr}\left(K_{pr}+10^5 m_2+10^5 m_r\right) &= Y_{pc}\left(K_{pc}+10^5 m_c\right), \quad and \\ Y_{pr}\left(K_{pr}+2x10^6 m_2+2x10^6 m_r\right) &= Y_{pc}\left(K_{pc}+2x10^6 m_c\right) \end{aligned} \tag{1.8}$$

If we set $Y_{pr} = Y_{pc}$ and $K_{pr} = K_{pc}$, Equations (1.8) become:

$$\begin{aligned} 10^5 m_2+10^5 m_r &= 10^5 m_c, \quad and \\ 2x10^6 m_2+2x10^6 m_r &= 2x10^6 m_c \end{aligned} \tag{1.9}$$

It can be seen from both relationships that $m_2 = m_c - m_r = 8.2x10^{-9} - 1.6x10^{-9} = 6.6x10^{-9}$ mg. So Equations (1.2) adapted to the Becks et al. supplemental experiments, admittedly in a non-unique way, may be written as Equations (1.10) after dividing through by the microbial masses (changed parameters in red.).

$$\frac{dn}{dt} = Dn_0 - \frac{\mu_{rn}}{Y_{rn}}\left[\frac{n(rm_r)}{K_{rn}+n}\right] - \frac{\mu_{cn}}{Y_{cn}}\left[\frac{n(cm_c)}{K_{cn}+n}\right] - Dn + pm_p\delta_p(EF)$$

$$\frac{dr}{dt} = \mu_{rn}\left[\frac{n(r)}{K_{rn}+n}\right] - \frac{\mu_{pr}((1.58E-6)r+0.842)}{Y_{pr}}\left[\frac{r(pm_p)}{K_{pr}+(6.6E-9)r+(rm_r)}\right] - Dr \qquad (1.10)$$

$$\frac{dc}{dt} = \mu_{cn}\left[\frac{n(c)}{K_{cn}+n}\right] - \frac{\mu_{pc}}{Y_{pc}}\left[\frac{c(pm_p)}{K_{pc}+(cm_c)}\right] - Dc$$

$$\frac{dp}{dt} = \mu_{pr}((1.58E-6)r+0.842)\left[\frac{p(rm_r)}{K_{pr}+(6.6E-9)r+(rm_r)}\right] + \mu_{pc}\left[\frac{p(cm_c)}{K_{pc}+(cm_c)}\right] - Dp - p\delta_p$$

In these equations, δ_p is the specific death rate for predators, which is recycled to nutrient at the efficiency "EF ≤ 1" in the 1st equation of set (1.10). Equations (1.10) also are subject to the parameter restraints, resulting from equations (1.7, 1.8 & 1.9), given by:

$$\mu_{rn} = \mathrm{k}\mu_{cn}$$
$$\mu_{pr} = \mu_{pc}$$
$$K_{pr} = K_{pc} \qquad (1.10a)$$
$$Y_{pr} = Y_{pc}$$

Now that the predators have been made to prefer rods over cocci with an increasing rod population, the rods are disadvantaged and would tend to die out. Based on numerical experiments, this is prevented by setting the "k" factor in the first of Equations (1.10a) to 1.5. As presented in Chapter 3, dimensionless forms of Equations (1.10) were developed also in order to aid

the numerical simulations of the Becks et al. experiments and the understanding of parameter interactions. These dimensionless equations may also serve as a basis for further study of a more abstract mathematical nature. They are also used in the Chapter 4 study of Shannon information theory applied to chaotic dynamics. Further details concerning the mathematical nature of the introduced preference change are given in the "Supplemental Information" at the end of this chapter.

1.3. Results.

Equations (1.10) were solved using MATLAB software (ODE45) subject to the initial conditions of n(0) = 0.03 mg/cc, r(0) = 4.2E6 cells/cc, c(0) = 1.0E6 cells/cc and p(0) = 3000 cells/cc. These should not be viewed as specifically-measured initial conditions, since such measurements were not made. However, several different initial conditions that were tested converged to the same system (strange) attractor. A set of parameters that produced chaotic dynamics is listed in Table 1.1

Based on parameter values selected in Kot et al. (1992) and value ranges given in Kravchenko et al. (2004), the Table 1.1 values appear reasonable in a physiological sense. Other than the dilution rate and mean microbe masses, we arrived at the remaining parameter values by trial and error coupled to numerical simulation experiments. With so many parameters necessary, and few measurements available, we think it would be potentially misleading to adapt a more formal parameter-fitting algorithm. However, a more detailed parameter sensitivity analysis may be found in Faybishenko, et al. (2018). This publication also describes in more detail the mathematical properties of the dynamics produced by Equations (1.10).

Table 1.1. Parameter values used in Equations (1.10) that yield chaotic dynamics with the dilution rate utilized in Becks et al. (2005).

D (hr^{-1})	n_0 (mg/cc)	μ_{rn} (hr^{-1})	Y_{rn}	K_{rn} (mg/cc)	μ_{cn} (hr^{-1})	Y_{cn}	K_{cn} (mg/cc)
0.0208	0.15	0.1873	0.4	0.009	0.1248	0.4	0.009
μ_{pr} (hr^{-1})	Y_{pr}	K_{pr} (mg/cc)	μ_{pc} (hr^{-1})	Y_{pc}	K_{pc} (mg/cc)	δ_p (hr^{-1})	m_r (mg)
0.05117	0.6	0.009	0.05117	0.6	0.009	0.00416	1.6E-9
m_c (mg)	m_p (mg)	EF	m_1 (cc)	i_1	m_2 (mg)	---	---
8.2E-9	3.2E-6	0.5	1.6E-6	0.8421	6.6E-9	---	---

The results of simulations, based on the parameter values listed in Table 1.1, are shown in Figures 1.2 and 1.3. Listed in Table 1.2 are the ranges of maximum Lyapunov exponents given in Becks et al. (2005), which are reasonably close to those calculated from our simulated time series. By varying D and other coefficients to keep the dimensionless forms of Equations (1.10) constant, it was possible to "tune" the Lyapunov exponents to be even closer to the experimental values. However, D was measured carefully in the experiments, so we decided to work only with those values.

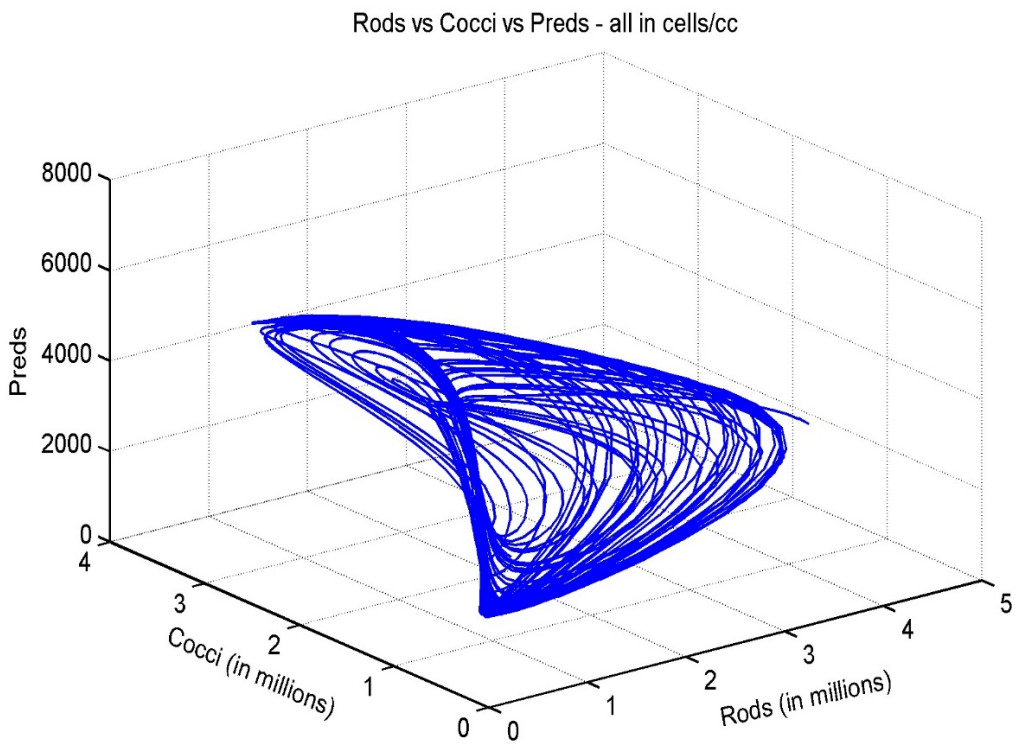

Figure 1.2. System-space (phase-space) plot of *r*(*t*), c(t) and p(t) for the parameters listed in Table 1.1 for D = 0.5/d (0.0208/hr) . A strange attractor is evident.

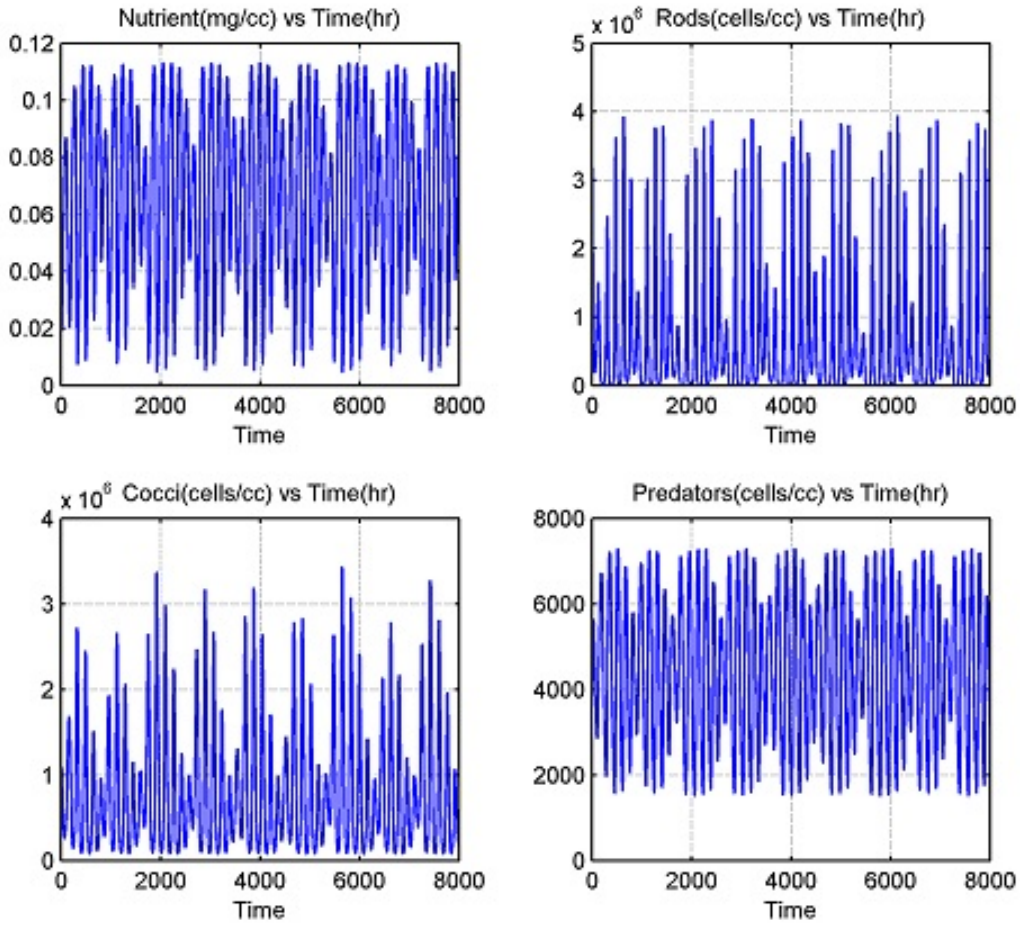

Figure 1.3. Irregular, non-periodic, dynamics of n(t), r(t), c(t) and p(t) associated with the system-space plot in Fig 1.2. By counting apparent concentration peaks, the mean frequency of the simulated data appears lower than that observed in Becks et al. [2005], but still within 50%. However, the mean model frequency can be selected by changing the dimensionless ratios of max specific growth and death rates to *D* (Chapter 3).

Table 1.2. Lyapunov exponents used to identify the presence of deterministic chaos based on the time series of concentrations shown in Figure 1.3 (Calculations were conducted using the R package "fractal" version: 2.0-1.)

Parameters	***n***	***r***	***c***	***p***
Time delay (hr.)	79	90	93	80
Largest Lyapunov exponent (hr^{-1})	0.085	0.016 (0.009-0.012)* Avg. = 0.011	0.004 (0.006-0.015)* Avg. = 0.01	0.015 (0.006-0.008)* Avg. = 0.007

Note *: range of maximum Lyapunov exponents determined by Becks et al. (2005).

As in the Becks et al. experiments, after obtaining chaotic dynamics at a dilution rate D=0.5/day (0.0208/hr), we decreased D to 0.45/day (0.01875/hr) with other parameters as listed in Table 1.1. It is shown in Figure 1.4 that the output starts in an irregular manner, and then becomes steady state with the cocci dying out. In the experiments, the results were periodic with all microbes surviving.

For a D value of 0.9/d (0.0375/hr), both simulations and experiments produced a classical steady state with one microbe dying out. However, the simulations resulted in the rods dying out, as shown in Figire1.5, while in the Becks et al. experiments the cocci died out. With this more classical result, it should be relatively easy to "fit" the model to the Becks et al. classical results. To illustrate this, we adjusted three parameters listed in Table 1.1. The maximum specific growth rate for the cocci was changed from 0.1248/hr to

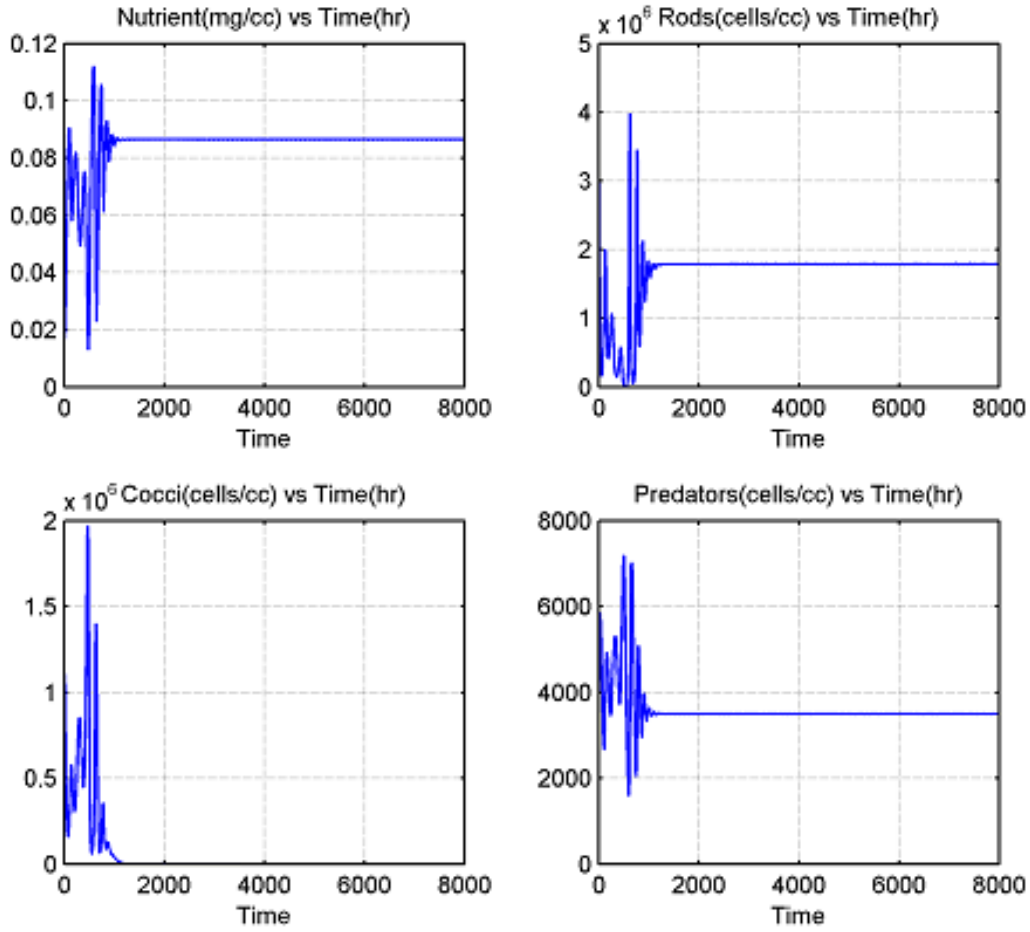

Figure 1.4. Resulting nutrient and microbe kinetics with D = 0.45/d (0.01875/hr.), as was done in the Becks et al. (2005) experiments.

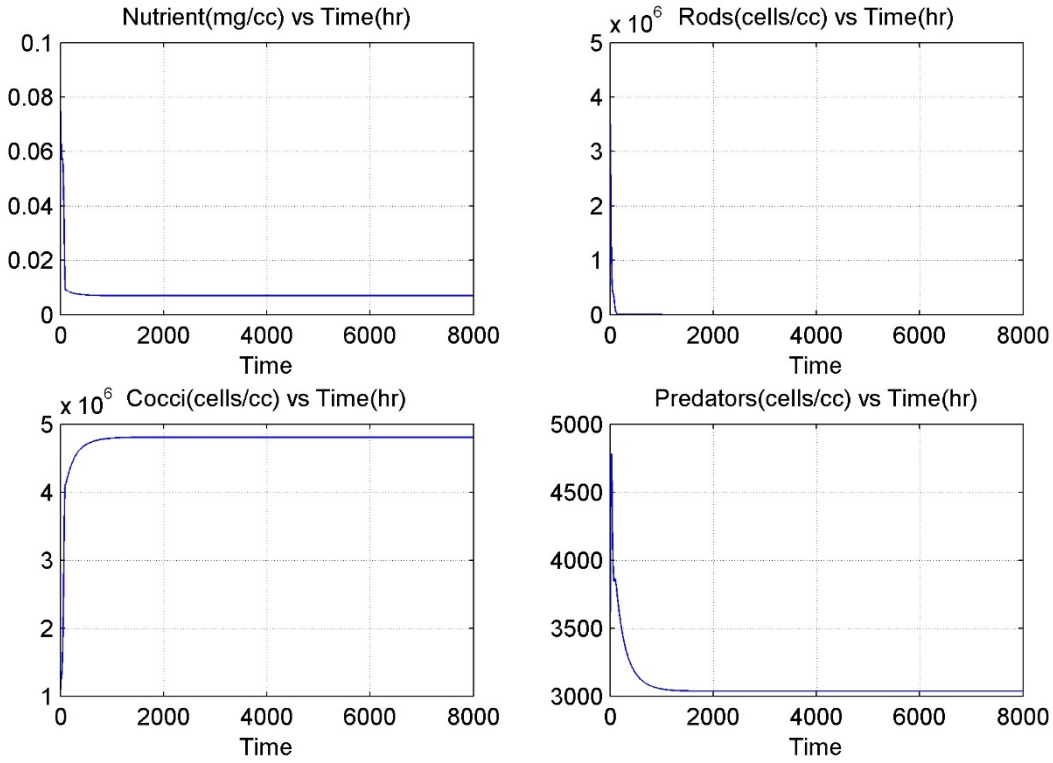

Figure 1.5. Resulting nutrient and microbe kinetics with *D* = 0.9/d (0.0375/hr).

0.1/hr., and the mean masses of the rods and predators were changed respectively from 1.6E-9 mg and 3.2E-6 mg to 2.2E-9 mg and 2.23E-6 mg. The resulting simulations shown in Figure 1.6, are essentially identical to the results in Becks et al. for D = 0.9/d (0.0375/hr). However, with these parameter values and D = 0.5/day the chaotic dynamics could not be reproduced.

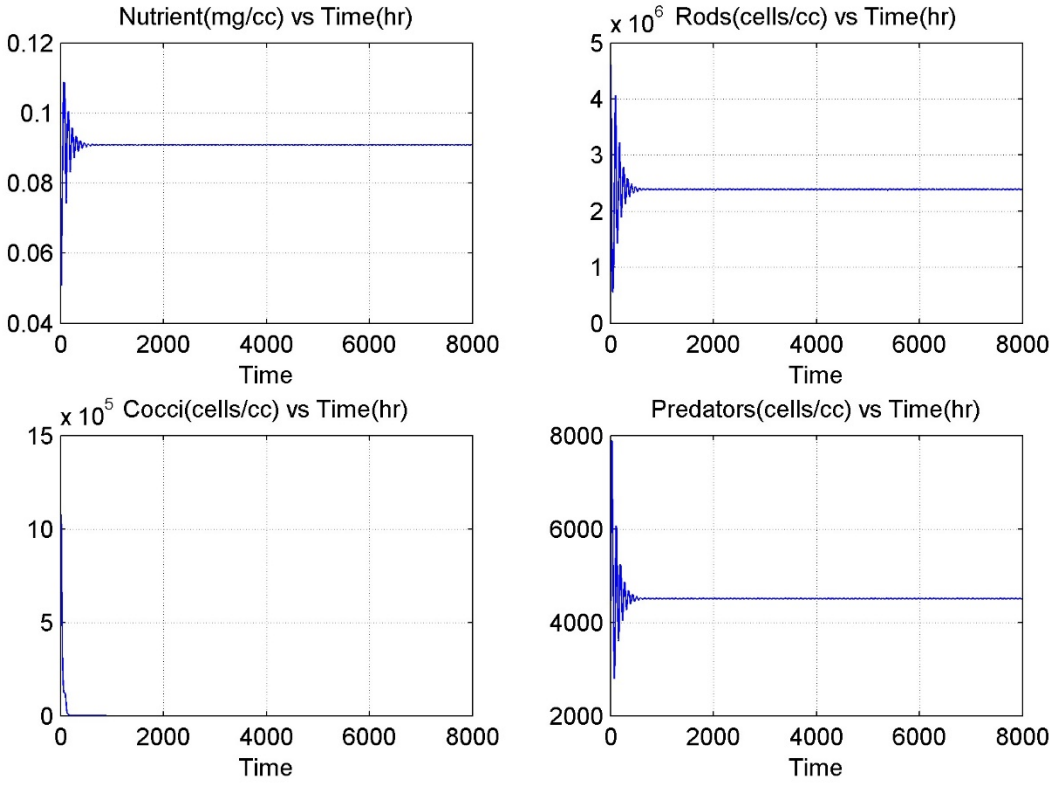

Figure 1.6. Simulated nutrient and microbe dynamics that match the Becks et al. [2005, Fig. 1] results for D = 0.9/d (0.0375/hr).

We also solved Equations (1.10) with D=0.75/d (0.03125/h.), which produced a classical steady-state with the rods dying out as shown in Figure 1.7; Becks et al. achieved a steady state also, but with all microbes surviving. Once again, similar but not identical.

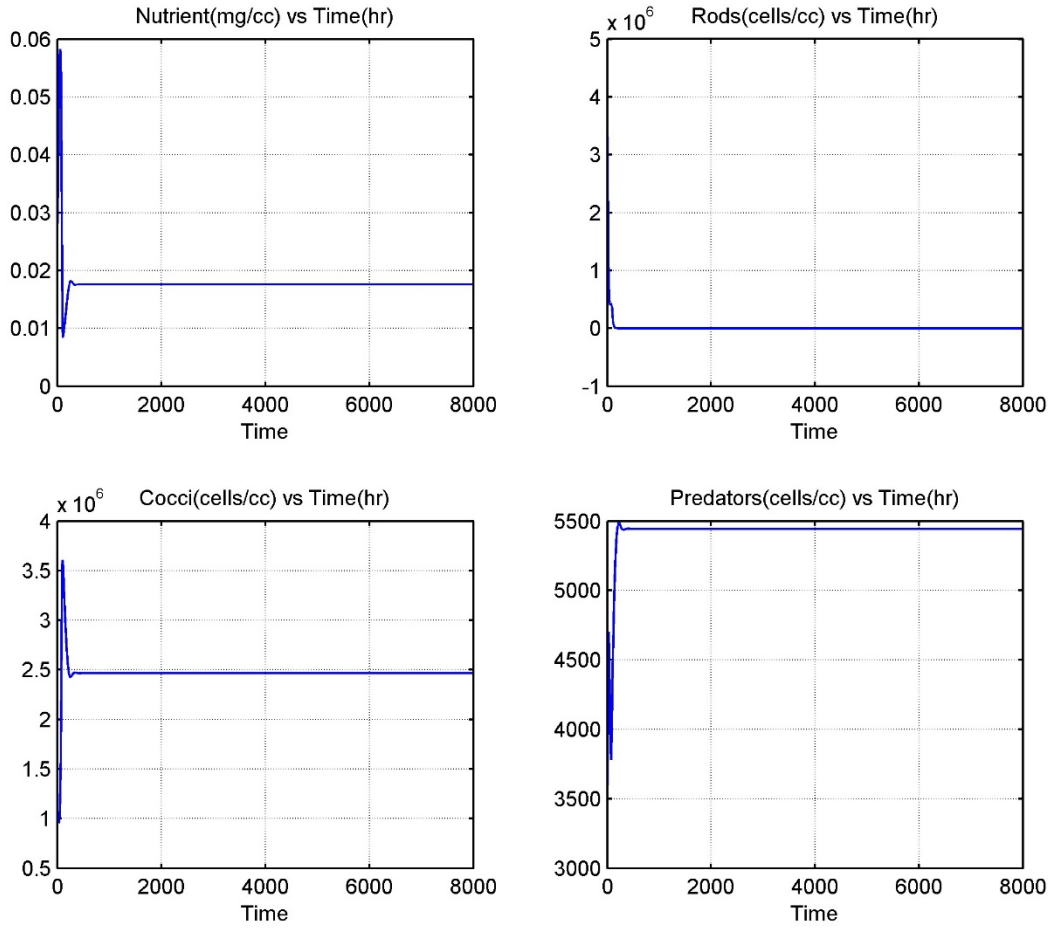

Figure 1.7. Resulting nutrient and microbe dynamics with D = 0.75/d (0.03125/h). Both the model and experiments produced classical steady states, but all microbes survived in the experiments while the rods died out in the model.

1.4. Discussion and Conclusions.

Clearly, the developed model with the mix of measured and selected parameters and coupling functions is not capturing all of the experimental details, and this would be expected with a chaotic/classical model having many unmeasured parameters and microbe coupling functions. What the results seem to be telling us is that future experiments should be designed to have a mix of modeling and testing so that the parameter values for the actual

experimental kinetics are better defined. This is a significant analytical and experimental challenge, but the need is also emphasized in the review paper by Fussmann (2007).

However, there were several interesting parallels between the experimental and model results. The nature and magnitudes of the model outputs were quite similar, and in one case they were made identical to the experimental results. At the dilution rate utilized by Becks et al. that resulted in chaotic dynamics, the experimental and simulated Lyapunov exponent values were in reasonable agreement. We therefore conclude that the availability of experimental results and a mathematical model, both producing classical and deterministic chaotic dynamics under similar conditions, is a useful first step that provides new insight that may lead to better understanding of complex phenomena in microbial systems and motivate further studies. From our viewpoint, the key methodology for obtaining internal chaotic dynamics was to cause the preference of *p* for *r* vs. *c* to vary with the *r* concentration, and to make *r* more competitive for nutrient than *c*, as well as to recycle some dying *p* biomass. This was also consistent with the experimental details, and it appears fortunate that Becks et al. (1995) had the foresight to perform the supplemental measurements related to food preferences and relative competitiveness of the various microbes. In this area our mathematical model suggests a prediction: *simulated chaotic dynamics required that the predator preference for rods versus cocci vary significantly with rod population density, and this could be checked experimentally using the Becks et al. (2005) measurement procedures with the microbe types used in their experiments*. (See Supplemental Information, page 27.)

The simulated deterministic chaos, and that of Becks et al., was purely a system-internal phenomenon; the feeding rates were maintained constant during each experiment, and external environmental effects were minimized by conducting experiments in the dark at constant temperature. In the simulations producing chaotic dynamics, all three microbes survived - what has been called previously a type of "sustainable state", with the concept of "state" represented by the strange attractor (Molz and Faybishenko, 2013). In the simulated non-chaotic cases, one microbe always died out, unless we imposed a microbe weakening with population growth, which added additional parameters to the model. So this aspect was not studied in depth. However, we were able to obtain a different type of chaotic dynamics driven by a sinusoidal feeding rate analogous to that produced in Kot et al. (1992) for a two-microbe system (See Chapter 2.).

Nonlinearity of natural microbial systems is the rule, because biological components (fluxes, plants, microbes, etc.), which are often represented by the dependent variables of system models and experiments, interact with each other in situation-dependent synergistic and/or antagonistic ways (feedbacks). When deterministic chaotic dynamics occur, the classical concept of ordered individual variation is lost, with time dependence becoming irregular, non-periodic and not predictable in the long term - hence the term "deterministic chaos." At least in a microbial system, however, a new type of order appears at the system level in the form of a time-persistent and bounded "strange attractor" in system (phase) space. Thinking about the attractor as representing the "full System", we don't perceive anything "chaotic", in the original meaning of the word, about such a structure. How this higher-level *system order* arises, and what is behind it in a

biophysical/chemical sense, needs to be studied further, which is a truly interdisciplinary problem involving biochemistry, irreversible thermodynamics, nonlinear dynamics and perhaps Shannon information theory (Schneider and Kay, 1994; Ben-Naim, 2008; Feistel and Ebling, 2011; Sagawa, 2014). The potential connection to information theory is intriguing, because anything described by a probability distribution has a Shannon measure of information (Ben-Naim, 2008), although the concept applies in its fullest sense only to discrete probability distributions. The statistical aspects of deterministic chaotic time series also have information measures, but classical steady or periodic states do not. This is a physical/mathematic difference between classical steady-states and the time-persistent states of deterministic chaos that may be fundamental. Based on a recent paper by Liepe et al. (2013), there is increasing interest in information concepts related to systems biology. Such material is discussed further in Chapter 4, which introduces some proposed information concepts related specifically to biological systems.

The mathematical model represented by Equations (1.2) or (1.10) may be generalized further in several ways. Additional microbes may be added, and the interaction kinetics may be modified to represent what is actually occurring in a given experiment. Such modification is not difficult in a formal mathematical sense; the challenge is to base such modifications on experimental evidence and motivation. Another interesting idea would be to perform experiments involving a spatial variable. This leads one to consider biofilms (Benefield and Molz, 1985). It is observed that nicely structured and controlled biofilms can be grown on electrodes, and electrical measurements can be made very precisely (Yoho et al., 2014). Finally one could extend the

Becks et al. (2005) supplemental experiments on predator preference change from 10^5 cells/cc to $4x10^6$ cells/cc to determine if there is a preference change and what the mathematical form is (Christofferson et al., 1997).

1.5. References.

1. Becks, L. and Arndt, H. 2008. Transitions from stable equilibria and back in an experimental food web. *Ecology 89*: 3222-3226.
2. Becks, L. and Arndt, H. 2009. Different types of synchrony in chaotic and cyclic communities. *Nature Communications 4*: doi:10.1038/ncommc2355.
3. Becks, L., Hilker, F., Malchow, H., Jürgens, K. and Arndt, H. 2005. Experimental demonstration of chaos in a microbial food web. *Nature 435***:** doi:10.1038/nature03627.
4. Benefield, L. and Molz, F. 1985. Mathematical simulation of a biofilm process. *Biotechnology and Bioengineering 27*: 921-931.
5. Beninca, E., Huisman, .J, Heerkloss, R., Johnk, K., Branko, P., Van Nes, E., Cheffer, M. and Ellner, S. 2008. Chaos in a long-term experiment with a plankton community. *Nature*: DOI:10.1038/NATURE06512.
6. Ben-Naim, A. 2008. *A Farewell to Entropy: Statistical Thermodynamics Based on Information*. World Scientific, London, UK.
7. Christofferson, K., Nybroe, O., Jurgens, K. and Hansen, M. 1997. Measurement of bacterivory by heterotrophic nano-flagellates using immunofluorescence labelling of ingested cells. *Aquatic Microbiology and Ecology*. 13, 127-134.
7. Costantino, R., Desharnais, F., Cushing, J. and Dennis B. 1997. Chaotic dynamics in insect population. *Science 275*: 389-391.

8. Faybishenko, B. and Molz, F. 2013. Nonlinear rhizosphere dynamics yields synchronized oscillations of microbial populations, carbon and oxygen concentrations induced by root exudation. *Procedia Environmental Sciences 19*: 369-378.
9. Faybishenko, B., Molz, F. and Agarwal, D. 2018. Nonlinear dynamics simulations of microbial ecological processes: Model diagnostic parameters of deterministic chaos and sensitivity analysis. In: Silvestrov, S., Malyarenko, A. and Rancic, M. (eds) *Stochastic Processes and Applications*. SPAS 2017. *Springer Proceedings in Mathematics and Statistics*, 271, pp. 437-486, Springer, Cham.
10. Feistel, R. and Ebling, W. 2011. *Physics of Self-organization and Evolution.* Wiley-VCH, Weimhein, GR.
11. Fussmann, G. 2007. Chaotic dynamics in food web systems, *in*, Blasius, Kurths and Stone, eds. Complex Population Dynamics: Nonlinear Modeling in Ecology, Epidemiology and Genetics. *World Scientific Lecture Notes in Complex Systems 7*: Chapter 1.
12. Graham, D., Knapp, C., Van Vleck, E., Bloor, K., Lane, T. and Graham, C. 2007. Experimental demonstration of chaotic instability in biological nitrification. *ISME Journal 1*: 385-393.
13. Hegger, R., Kantz, H. and Schreiber, T. 1999. Practical implementation of nonlinear time series methods: The TISEAN package. *Chaos 10*: 413-421.
14. Kot, M., Sayler, G. and Schultz T. 1992. Complex dynamics in a model microbial system. *Bulletin of Mathematical Biology 54*: 619-648.
15. Kravchenko, L., Strigl, N. and Shvytov, I. 2004. Mathematical simulation of the dynamics of interacting populations of rhizosphere microorganisms. *Microbiology 73*: 189-195.

16. Liepe, J., Filippi, S., Komorowski, M. and Stumpf, M. 2013. Maximizing the information content of experiments in systems biology. *PLOS Computational Biology 9*: e1002888.
17. Molz, F. and Faybishenko, B. 2013. Increasing evidence for chaotic dynamics in the soil-plant-atmosphere system: A motivation for future research. *Procedia Environmental Sciences 19*: 681-690.
18. Rosenstein, M., Collins, J. and De Luca, C. 1993. A practical method for calculating largest Lyapunov exponent from small data sets. *Physica D 65*: 117-124.
19. Sagawa, T. 2014. *Thermodynamics of Information Processing in Small Systems*. Springer Theses, Berlin GR.
20. Schneider, E. and Kay, J. 1994. Life as a manifestation of the second law of thermodynamics. *Math. Comput. Modeling 19*: 25-48.
21. Yoho, R., Popat, S. and Torres, C. 2014. Dynamic potential-dependent electron transport pathway shifts in anode biofilms of *Geobacter sulfurreducens*. *Chem. Sus. Chem.* ***7***: 3413-3419.

S1. Supplemental Information Concerning Predator Preference Change.

Based on unmodified Monod kinetics, the uptakes of r and c by P in cells per hour is given by

$$\frac{dr_p}{dt} = \frac{pm_p\mu_{pr}r}{Y_{pr}(K_{pr} + m_r r)} \quad and \quad \frac{dc_p}{dt} = \frac{pm_p\mu_{pc}c}{Y_{pc}(K_{pc} + m_c c)} \tag{S1}$$

We modified this to make the uptake rates on a cellular basis equal at r = c = 1E5, and to have r uptake 4 times faster than c uptake at r = c = 2.0E6. To do this, μ_{pr} and K_{pr} were made linear functions of r, i.e. $\mu_{pr} = \mu_{pr}(m_1 r + i_1)$ and $K_{pr} = K_{pr} + m_2 r$. This resulted in:

$$\frac{dr_p}{dt} = \frac{pm_p \mu_{pr}(m_1 r + i_1) r}{Y_{pr}(K_{pr} + m_2 r + m_r r)} \tag{S2}$$

The ratio of $(\frac{dr_p}{dt})/(\frac{dc_p}{dt})$ is now given by:

$$\frac{pm_p \mu_{pr}(m_1 r + i_1) r}{Y_{pr}(K_{pr} + m_2 r + m_r r)} \left(\frac{Y_{pc}(K_{pc} + m_c c)}{pm_p \mu_{pc} c} \right) \tag{S3}$$

Applying the conditions on r and c at 1E5 and 2.0E6 resulted in m_1 = 1.597E-6, i_1 = 0.8421 and $m_2 = m_c - m_r$. In addition, it was required that

$$\mu_{pr} = \mu_{pc}, \quad K_{pr} = K_{pc} \text{ and } \quad Y_{pr} = Y_{pc} \tag{S4}$$

When all this is substituted in (S3) with the condition that r = c, one obtains

$$\frac{pm_p \mu_{pr}(1.579E-6 r + 0.8421) r}{Y_{pr}(K_{pr} + (m_c - m_r) r + m_r r)} \left(\frac{Y_{pr}(K_{pr} + m_c r)}{pm_p \mu_{pr} r} \right) \tag{S5}$$

Most terms cancel, and the final simple and clear result is:

$$Ratio(r) = \left(\frac{dr_p}{dt} \right) / \left(\frac{dc_p}{dt} \right) = m_1 r + i_1 = (1.579E-6) r + 0.8421 \tag{S6}$$

Ratio(1E5) = 1 and *Ratio(2E6)* = 4, with a linear variation with r. So whenever r and c are at the same cell densities, the uptake rate ratio is given by (S6). Becks et al. measured this ratio at one r and c value and got 4. But it could be done at a variety of values to see if (S6) is approximately valid, or if there is some other type of variation, or perhaps no variation. We would actually expect some other type of variation, but any type of predator preference change for r vs c could be an important part of the overall dynamics. It would illustrate how potential couplings can be complex beyond any of the classical kinetic expressions. The applicable experimental technical was developed some time ago by Christofferson et al. (1997.)

Chapter2: Further Study of the Becks et al. Equations.

2.1. Introduction.

As given in Chapter 1, straight generalization of the Kot et al (1992) system results in

$$\begin{aligned}
\frac{dn}{dt} &= Dn_0 - \frac{\mu_{rn}}{Y_{rn}}\left[\frac{n(rm_r)}{K_{rn}+n}\right] - \frac{\mu_{cn}}{Y_{cn}}\left[\frac{n(cm_c)}{K_{cn}+n}\right] - Dn \\
\frac{d(rm_r)}{dt} &= \mu_{rn}\left[\frac{n(rm_r)}{K_{rn}+n}\right] - \frac{\mu_{pr}}{Y_{pr}}\left[\frac{(rm_r)(pm_p)}{K_{pr}+(rm_r)}\right] - D(rm_r) \\
\frac{d(cm_c)}{dt} &= \mu_{cn}\left[\frac{n(cm_c)}{K_{cn}+n}\right] - \frac{\mu_{pc}}{Y_{pc}}\left[\frac{(cm_c)(pm_p)}{K_{pc}+(cm_c)}\right] - D(cm_c) \qquad (2.1) \\
\frac{d(pm_p)}{dt} &= \mu_{pr}\left[\frac{(rm_r)(pm_p)}{K_{pr}+(rm_r)}\right] + \mu_{pc}\left[\frac{(cm_c)(pm_p)}{K_{pc}+(cm_c)}\right] - D(pm_p)
\end{aligned}$$

The parameters involved are maximum specific growth rates (μ), half saturation constants (*K*) and yield coefficients (*Y*), a total of twelve. The actual parameter values that applied to the Becks et al. experiments are not known in detail, so the initial objective was to study the properties of model (2.1) using the experiments as a guide. (We elected to work with the equations in dimensional form, because (like us) we thought most readers would find it easier to maintain a physical feel for what might be happening. Dimensionless results may be found in Chapter 3) A convenient and reasonable set of values for starting this process, similar to those selected by Kot et al.(1992) are given in Table 2.1. Initial conditions were selected as n(0) = 0.03 mg/cc, r(0) =

$4.2x10^6$ cells/cc, $c(0) = 10^6$ cells/cc and $p(0) = 3000$ cells/cc. These are in the range of values observed in the Becks et al. experiments, but they should not be viewed as specifically-measured initial conditions. Many other initial conditions give sensible results.

Table 2.1. Parameter values selected for an initial mathematical analysis of the Becks et al. experiments using the generalized Kot et al. Model (2.1). Units for "μ" are hr^{-1}, for "*K*" are mg/cc, and "*Y*" are mg/mg. Microbial masses are held constant at the values given (mg) in Chapter 1.

μ_{rn}	μ_{cn}	μ_{pr}	μ_{pc}	K_{rn}	K_{cn}	K_{pr}	K_{pc}	Y_{rn}	Y_{cn}		Y_{pr}	Y_{pc}
0.7	0.65	0.211	0.246	0.008	0.009	0.019	0.009	0.4	0.4		0.6	0.6

For reasonable parameter values, Equations (2.1) would not yield a stable solution having non-zero values for all dependent variables. The common behavior was either for the rods to die out, leaving only cocci and predators, or for the cocci to die out, leaving only rods and predators. Less than 1% changes in the controlling parameters could flip the system from all *c*, *n* and *p* to all *r*, *n* and *p*, or vice-versa. Therefore, if the full system being simulated is defined as a finite, varying mixture of nutrient, rods, cocci and predators, as observed in most of the Becks et al. experiments, one could say that Equations (2.1), due to die-offs of rods or cocci, do not yield a stable, long-term, four-variable solution. For this reason, it was decided to modify the model as follows.

2.2. Another Model Generalization.

Many organisms weaken somewhat with success, and are also subject to a natural death rate—the so-called intrinsic death rate. In addition, the

biomass of dead microbes becomes a new nutrient source, so the death of a relatively large predator could provide nutrient for many relatively small cocci or rods. This process is called biomass recycling to nutrient. All three potential processes, weakening with success, intrinsic death rates and biomass recycling are taken into account in Model 2.2: (New terms in red.)

$$\frac{dn}{dt}=Dn_0-\frac{\mu_{rn}[1-S_{rn}m_r r]}{Y_{rn}}\left[\frac{n(rm_r)}{K_{rn}+n}\right]-\frac{\mu_{cn}[1-S_{cn}m_c c]}{Y_{cn}}\left[\frac{n(cm_c)}{K_{cn}+n}\right]-Dn+pm_p\partial_p(EF)$$
$$+[rm_r\delta_r+cm_c\delta_c+pm_p\delta_p]EF$$
$$\frac{dr}{dt}=\mu_{rn}[1-S_{rn}m_r r]\left[\frac{n(r)}{K_{rn}+n}\right]-\frac{\mu_{pr}[1-S_{pr}m_p p]}{Y_{pr}}\left[\frac{r(pm_p)}{K_{pr}+rm_r}\right]-r\delta_r-Dr \qquad (2.2)$$
$$\frac{dc}{dt}=\mu_{cn}[1-S_{cn}m_c c]\left[\frac{n(c)}{K_{cn}+n}\right]-\frac{\mu_{pc}[1-S_{pc}m_p p]}{Y_{pc}}\left[\frac{c(pm_p)}{K_{pc}+cm_c}\right]-c\delta_c-Dc$$
$$\frac{dp}{dt}=\mu_{pr}[1-S_{pr}m_p p]\left[\frac{rm_r(p)}{K_{pr}+rm_r}\right]+\mu_{pc}[1-S_{pc}m_p p]\left[\frac{cm_c(p)}{K_{pc}+cm_c}\right]-p\delta_p-Dp$$

The terms in Equations (2.2) containing slopes "S_{ij}" cause a small linear decrease of the maximum specific growth rates as microbe mass concentrations increase, and the "δ" terms represent the specific (intrinsic) death rates for each microbe. The last term in the nutrient equation (1st Equation of (2.2)) sums the dying biomass and converts it to nutrient with conversion efficiency "EF". The eight additional selected parameter values are listed in Table 2.2, with specific death rates for rods and cocci not needed.

Table 2.2. New parameters in Equations (2.1), and a set of test values. Units of "S" are mg^{-1}, units of the specific death rates "δ" are hr^{-1}, and $0 \le EF \le 1$ is dimensionless.

S_{rn}	S_{cn}	S_{pr}	S_{pc}	δ_r	δ_c	δ_p	EF
50.0	1.0	1.0	1.0	0.0	0.0	0.02	0.5

2.3. Results.

Using MATLAB software, for the parameter values listed in Tables 2.1 and 2.2, we solved Equations (2.2) for a dilution rate $D = 0.1\ \text{hr}^{-1}$, and an inflowing nutrient concentration $n_0 = 0.15$ mg/cc. Dependent variables (n, r, c, and p) as functions of time are presented in Figure 2.1.

All the microbes now exist together, and the overall solutions are periodic. Many test runs with different parameters have shown much more stable behavior of the dependent variables, so we are observing the situation in which added model nonlinearity causes increased system-wide stability. The situation when the most abundant microbes are weakened leads to evolutionary dynamics of specific predator-prey pairs, which oscillate in time similar to those predicted by the classical Lotka-Volterra equations, and which are also called "Kill-the-Winner" systems (Bratbak et al., 1990;; Rohwer and Barott, 2012). At this point, the problem we experienced was that regardless of the selected parameter values, chaotic dynamics would not occur. This was shown to be true rigorously by Kot et al. in their three-variable study, before inducing chaotic dynamics by making the feeding rate periodic. So we decided to try this in our system by replacing the inflowing nutrient concentration [$n_0 = 0.15$] with [$n_0 = 0.15(1 - 0.5\sin(0.52t))$], which represents a sinusoidal variation about 0.15 mg/cc with an amplitude of 0.075 and a period of 12 hr. The resulting dynamics shown in Figures 2.2 and 2.3 appear analogous to that observed by Kot et al. (1992) in their three-variable system with a sinusoidal feeding rate given by $0.155(1+0.6\sin(0.262t))$ in our units. The diagnostic

parameters for the nonlinear concentration time series shown in Figure 2.3 are summarized in Table 2.3.

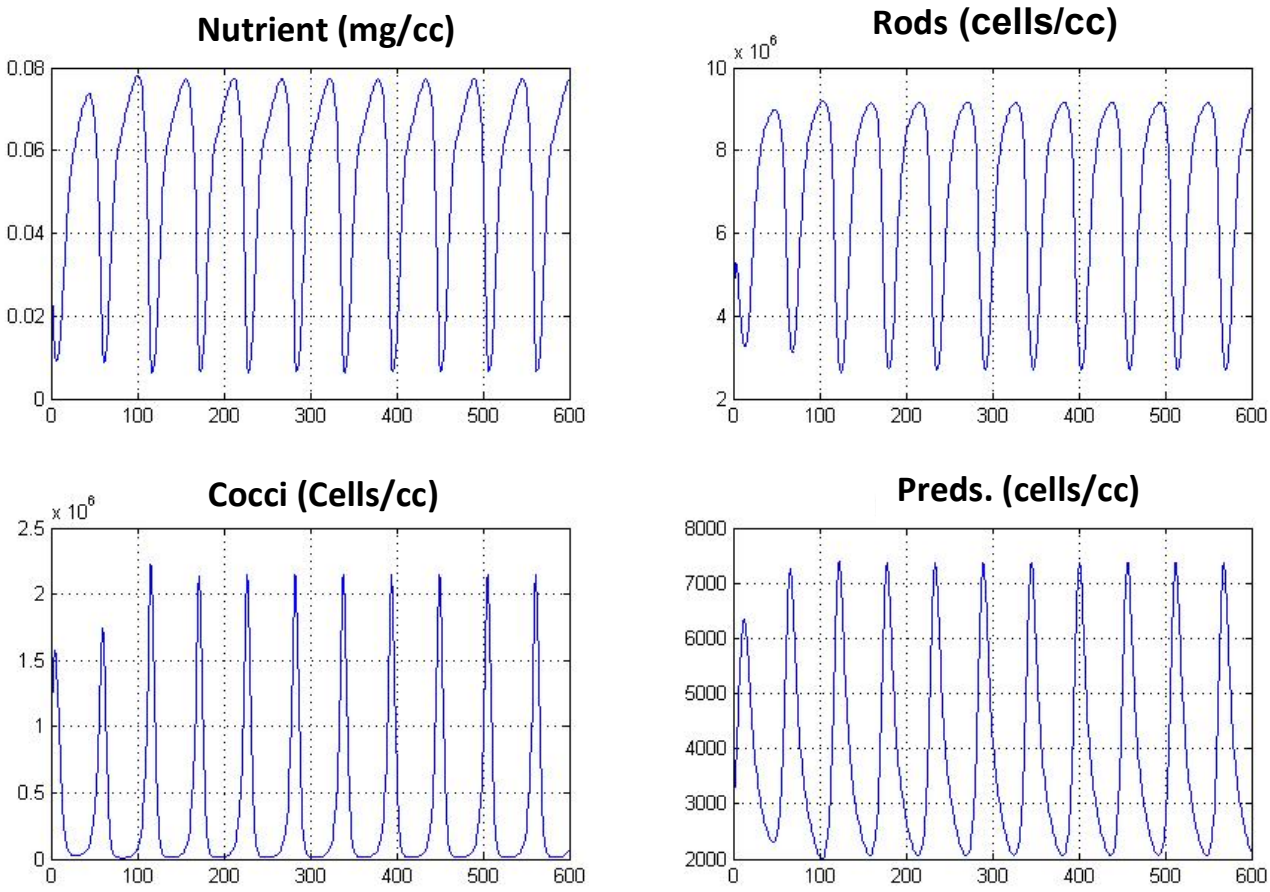

Figure 2.1. Nutrient mass concentrations and microbial cell number concentrations as functions of time (hr.). With the modified Equations (2.2), it is now relatively easy to produce stable periodic oscillations of concentrations of all three microbes.

Table 2.3. Diagnostic nonlinear dynamics parameters used to identify the presence of deterministic chaos based on the time series of concentrations shown in Figures 2.2 and 2.3. (Note: Analysis using R software packages "FRACTAL").

Parameters	**n**	**r**	**c**	**p**
Time delay (hr.)	18	56	69	62
Correlation dimension d2	1.97	0.91	1.75	1.08
Embedding dimension	4	2	2	2
Information dimension d1	2.22	1.42	1.28	1.65
Largest Lyapunov exp. (hr^{-1})	0.28	0.41	0.40	0.40
Sum of Lyapunov exponents	-1.40	-0.16	~ 0	~0
Hurst exponent	0.527	0.637	0.552	0.642

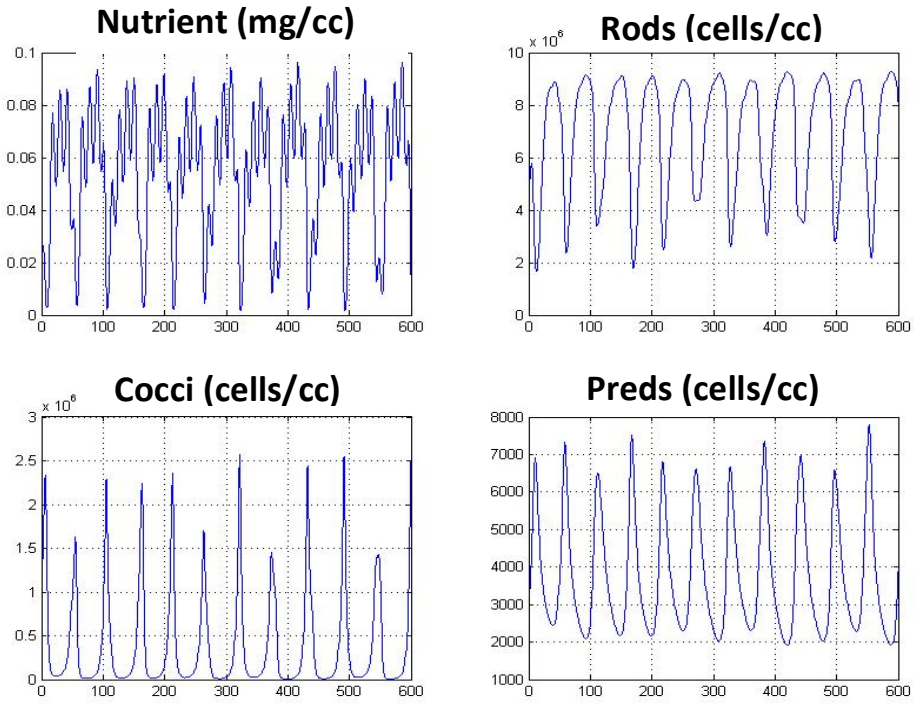

Figure 2.2. Plots of nutrient and microbes as functions of time resulting from a solution of Equations (2.2), using parameter values specified in Tables 2.1 and 2.2, along with a sinusoidal, 12 hr. period, feeding rate. The only parameter difference with the solution shown in Figure 2.1 is the sinusoidal feeding rate.

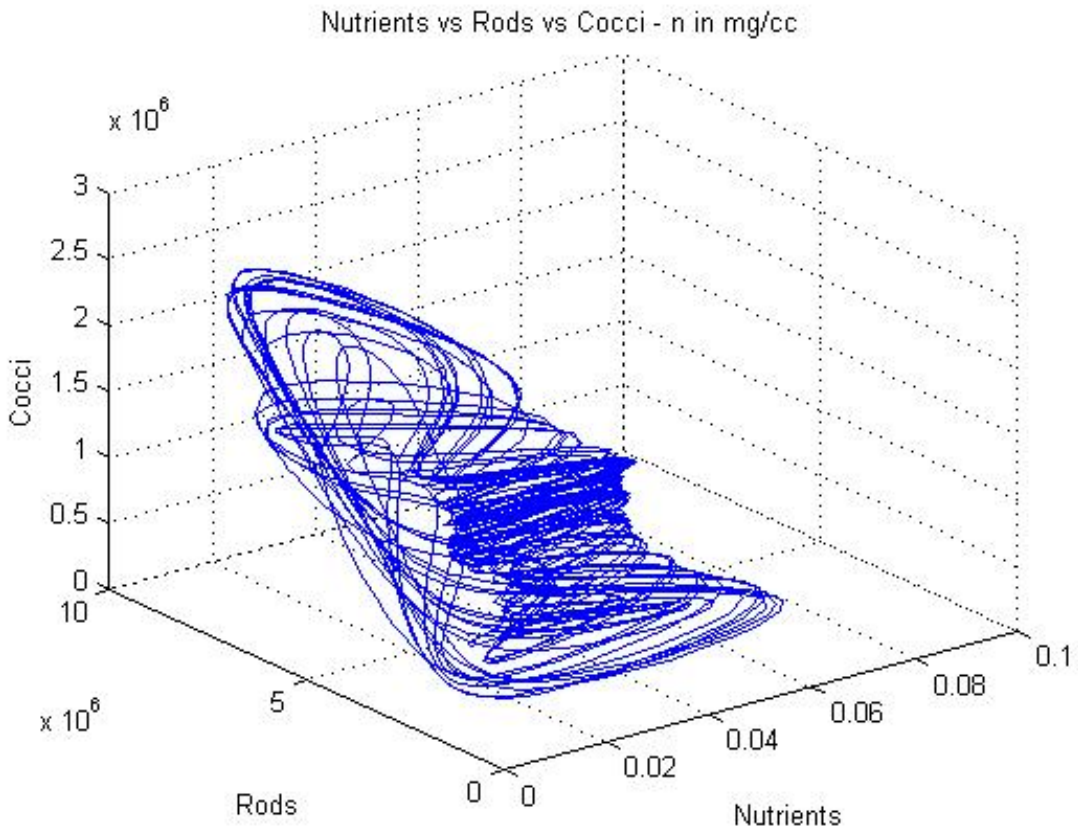

Figure 2.3. 3-D system space plots of Equations (4) solution with an inflowing nutrient concentration given by $Dn_0 = [0.15(1 - 0.5\sin(0.52t))]$. A strange attractor is evident.

2.4. Conclusions.

We did not further pursue the time-dependent feeding rate solutions, because the feeding rate was held constant in the Becks et al. (2005) experiments that were conducted in the dark at constant temperature. So, the chaotic dynamics obtained was strictly an internal process. The idea of microbe weakening with population growth was dropped also because of the added parameters involved. Instead we focused on better implementation of the results of the supplemental experiments involving predator preference for rods versus cocci and the ability of rods to out-compete cocci for food under starvation conditions. It is entirely possible, however, that the inclusion of microbe weakening with population growth could result in an overall formulation that is superior in some way, so this possibility should be examined in future research.

2.5. References.

1. Becks, L., Hilker, F., Malchow, H., Jürgens, K. and Arndt, H. 2005. Experimental demonstration of chaos in a microbial food web. *Nature Letters 435*: doi:10.1038/nature03627.
2. Bratbak, G., Heldal, M., Norland, S. and Thingstad, T. 1990. Viruses as partners in spring bloom microbial trophodynamics. *Appl Environ Microbiol 56*: 1400-1405.
3. Kot, M., Sayler, G. and Schultz T. 1992. Complex dynamics in a model microbial system. *Bulletin of Mathematical Biology 5*4: 619-648.
4. Rohwer, F. and Barott K. 2013. Viral information. *Biol Philos 28*: 283–297. doi 10.1007/s10539-012-9344-0.

5. Strigul, N. and Kravchenko, L. 2006. Mathematical modeling of PGPR inoculation in the rhizosphere. *Environ Mod & Softwr 21*: 1158-1164

Chapter 3. Dimensionless Forms for Equations (1.10).

3.1. Introduction.

While exploring the nature and implications of coupled, nonlinear, equation systems, it is often enlightening to put the equations in non-dimensional form – as was done by Kot et al. (1992). Such a formulation has obvious advantages for a more general mathematical analysis beyond that presented in this report. However, we did use dimensionless equations to better understand parameter interactions, and to further check the consistency of our formulations.

3.2. Dimensionless Formulation.

Equations (1.10) may be written as:

$$\frac{dn}{dt} = Dn_0 - r(m_r)\left[\frac{\mu_{rn}}{Y_{rn}}\left(\frac{n}{K_{rn}+n}\right)\right] - c(m_c)\left[\frac{\mu_{cn}}{Y_{cn}}\left(\frac{n}{K_{cn}+n}\right)\right] - Dn + pm_p\delta_p EF$$

$$m_r\frac{dr}{dt} = r(m_r)\left[\mu_{rn}\left(\frac{n}{K_{rn}+n}\right)\right] - \frac{\mu_{pr}\left(m_1 r + i_1\right)}{Y_{pr}}\left(\frac{r(m_r)}{K_{pr}+m_2 r + r(m_r)}\right)p(m_p) - Dr(m_r)$$

$$m_p\frac{dp}{dt} = c(m_c)p(m_p)\left[\left[\mu_{pr}\left(\frac{n}{K_{cn}+n}\right)\right]\left(\frac{\mu_{pc}}{Y_{pr}}\right)\left(\frac{r(m_r)}{K_{pr}+m_2 r + r(m_r)}\right) + \mu_{pc}\left(\frac{c(m_c)}{K_{pc}+c(m_c)}\right)\right] - Dp(m_p) - p(m_p)\delta_p \quad (3.1)$$

Following the lead of Kot et al. (1992), we define the dimensionless variables given by:

$$w = \frac{n}{n_0}, \quad x = \frac{rm_r}{Y_{rn} n_0}, \quad y = \frac{cm_c}{Y_{cn} n_0}, \quad z = \frac{pm_p}{Y_{rn} Y_{cn} Y_{pr} Y_{pc} n_0} \quad and \quad \tau = Dt \tag{3.1a}$$

This results in the substitutions listed in (I-1b):

$$n = n_0 w, \quad rm_r = x Y_{rn} n_0, \quad cm_c = y Y_{cn} n_0, \quad pm_p = z Y_{rn} Y_{cn} Y_{pr} Y_{pc} n_0 \quad and \quad t = \tau / D, \tag{3.1b}$$

which yields the equation set:

$$D n_0 \frac{dw}{d\tau} = D n_0 - x Y_{rn} n_0 \left[\frac{\mu_{rn}}{Y_{rn}} \left(\frac{n_0 w}{K_{rn} + n_0 w} \right) \right] - y Y_{cn} n_0 \left[\frac{\mu_{cn}}{Y_{cn}} \left(\frac{n_0 w}{K_{cn} + n_0 w} \right) \right] - D n_0 w + z Y_{rn} Y_{cn} Y_{pr} Y_{pc} n_0 \delta_p EF$$

$$D Y_{rn} n_0 \frac{dx}{d\tau} = x(Y_{rn} n_0) \left[\mu_{rn} \left(\frac{n_0 w}{K_{rn} + n_0 w} \right) \right] +$$

$$- \frac{\mu_{pr} (m_1 x Y_{rn} n_0 / m_r + i_1)}{Y_{pr}} \left(\frac{x(Y_{rn} n_0)}{K_{pr} + m_2 x Y_{rn} n_0 / m_r + x(Y_{rn} n_0)} \right) z Y_{rn} Y_{cn} Y_{pr} Y_{pc} n_0 - D x(Y_{rn} n_0) \tag{3.2}$$

$$D \frac{dz}{d\tau} = \frac{dy}{d\tau} \frac{\mu_{PR}}{Y_{pr}} (m_1 x Y_{rn} n_0 / m_r + i_1) \left[\mu_{cn} \left(\frac{n_0 w}{K_{cn} + n_0 w} \right) \right] \frac{x(Y_{rn} n_0)}{K_{pc} + m_2 x Y_{rn} n_0 / m_r + x(Y_{rn} n_0)} + z \mu_{rn} \left(\frac{y(Y_{cn} n_0)}{K_{pc} + y(Y_{cn} n_0)} \right) - D y(Y_{cn} n_0) - z \delta_p$$

Further simplification results in:

$$\frac{dw}{d\tau} = 1 - \frac{\mu_{rn}}{D}\left(\frac{wx}{K_{rn}/n_0 + w}\right) - \frac{\mu_{cn}}{D}\left(\frac{wy}{K_{cn}/n_0 + w}\right) - w + \frac{zY_{rn}Y_{cn}Y_{pr}Y_{pc}\delta_p EF}{D}$$

$$\frac{dx}{d\tau} = \frac{\mu_{rn}}{D}\left(\frac{wx}{K_{rn}/n_0 + w}\right) - \frac{\mu_{pr}(m_1 Y_{rn} n_0)}{m_r}\frac{Y_{cn}Y_{pc}}{D}\left(\frac{x^2 z}{K_{pr}/(Y_{rn}n_0) + x(m_2/m_r + 1)}\right) +$$
$$-\frac{\mu_{pr} i_1 Y_{cn} Y_{pc}}{D}\left(\frac{xz}{K_{pr}/(Y_{rn}n_0) + x(m_2/m_r + 1)}\right) - x$$

$$\frac{dz}{d\tau} = \frac{\mu_{pr} m_1 Y_{rn} n_0}{\mu_{cn} D m_r}\left(\frac{wy}{K_{cn}/n_0 + w}\right) - \frac{\mu_{pc} x^2 z Y_{rn} Y_{pr}}{D}\left(\frac{yz}{K_r/(Y_{cn}n_0) + y}\right) + \frac{\mu_{pr} i_1}{D}\left(\frac{xz}{K_{pr}/Y_{rn}n_0 + x(m_2/m_r + 1)}\right) \quad (3.3)$$
$$+\frac{\mu_{pc}}{D}\left(\frac{yz}{K_{pc}/Y_{cn}n_0 + y}\right) - z(1 + \frac{\delta_p}{D})$$

Defining the dimensionless parameters (3.4), and substituting in (3.3) results in the dimensionless equation set (3.5):

$$A1 = \frac{\mu_{rn}}{D}; a1 = \frac{K_{rn}}{n_0}; B_1 = \frac{\mu_{cn}}{D}; \text{b1} = \frac{K_{cn}}{n_0}; C1 = Y_{rn}Y_{cn}Y_{pr}Y_{pc}\frac{\delta_p}{D}EF \qquad \rightarrow w\,eq.$$

$$A1 = \frac{\mu_{rn}}{D}; a1 = \frac{K_{rn}}{n_0}; B_2 = \frac{\mu_{pr}m_1Y_{rn}n_0Y_{cn}Y_{pc}}{Dm_r}; b2 = \frac{(K_{pr})}{Y_{rn}n_0}$$

$$b2a = \frac{m_2}{m_r} + 1; C2 = \frac{\mu_{pr}i_1Y_{cn}Y_{pc}}{D}; b2 = \frac{(K_{pr})}{Y_{rn}n_0}; b2a = \frac{m_2}{m_r} + 1 \qquad \rightarrow x\,eq.$$

$$B1 = \frac{\mu_{cn}}{D}; \text{b1} = \frac{K_{cn}}{n_0}; B3 = \frac{\mu_{pc}Y_{rn}Y_{pr}}{D}; b3 = \frac{K_{pc}}{Y_{cn}n_0} \qquad \rightarrow y\,eq. \qquad (3.4)$$

$$A4 = \frac{\mu_{pr}m_1Y_{rn}n_0}{Dm_r}; b2 = \frac{K_{pr}}{Y_{rn}n_0}; b2a = \frac{m_2}{m_r} + 1; \text{B4} = \frac{(\mu_{pr}i_1)}{D}; b2 = \frac{K_{pr}}{Y_{rn}n_0}$$

$$b2a = \frac{m_2}{m_r} + 1; \text{C4} = \frac{\mu_{pc}}{D}; b3 = \frac{K_{pc}}{Y_{cn}n_0}; D4 = 1 + \frac{\delta_p}{D} \qquad \rightarrow z\,eq.$$

$$\frac{dw}{d\tau} = 1 - A1\left(\frac{wx}{a1 + w}\right) - B1\left(\frac{wy}{b1 + w}\right) - w + C1(z)$$

$$\frac{dx}{d\tau} = A1\left(\frac{wx}{a1 + w}\right) - B2\left(\frac{x^2z}{b2 + x(b2a)}\right) - C2\left(\frac{xz}{b2 + x(b2a)}\right) - x \qquad (3.5)$$

$$\frac{dy}{d\tau} = B1\left(\frac{wy}{b1 + w}\right) - B3\left(\frac{yz}{b3 + y}\right) - y$$

$$\frac{dz}{d\tau} = A4\left(\frac{x^2z}{b2 + x(b2a)}\right) + B4\left(\frac{xz}{b2 + x(b2a)}\right) + C4\left(\frac{yz}{b3 + y}\right) - D4(z)$$

3.3. Example Solution to the Dimensionless Equations.

Substituting the numerical parameter values in Table (1.1) into the derived dimensionless parameters results in the equation set (3.6)

$$\frac{dw}{d\tau} = 1. - 9.0048\left(\frac{wx}{0.06+w}\right) - 6.\left(\frac{wy}{0.06+w}\right) - w + 0.0058(z)$$

$$\frac{dx}{d\tau} = 9.0048\left(\frac{wx}{0.06+w}\right) - 35.4254\left(\frac{x^2 z}{0.15+x(5.125)}\right) - 0.4972\left(\frac{xz}{0.15+x(5.125)}\right) - x \qquad (3.6)$$

$$\frac{dy}{d\tau} = 6.\left(\frac{wy}{0.06+w}\right) - .5904\left(\frac{yz}{0.15+y}\right) - y$$

$$\frac{dz}{d\tau} = 147.61\left(\frac{x^2 z}{0.15+x(5.125)}\right) + 2.0716\left(0\frac{xz}{.15+x(5.125)}\right) + 2.46\left(\frac{yz}{0.15+y}\right) - 1.2(z)$$

Equations (3.6) were solved with slightly different initial conditions, because we wanted all points to fall on the strange attractor right from the beginning as a basis for the following Chapter 4 dealing with Shannon Information Theory. So an attractor starting point given by w = 0.579, x = 0.0193, y = 0.0516 and z = 1.079 was utilized.

3.4. Results and Discussion.

Results are given in Figures 3.1, 3.2 and 3.3.

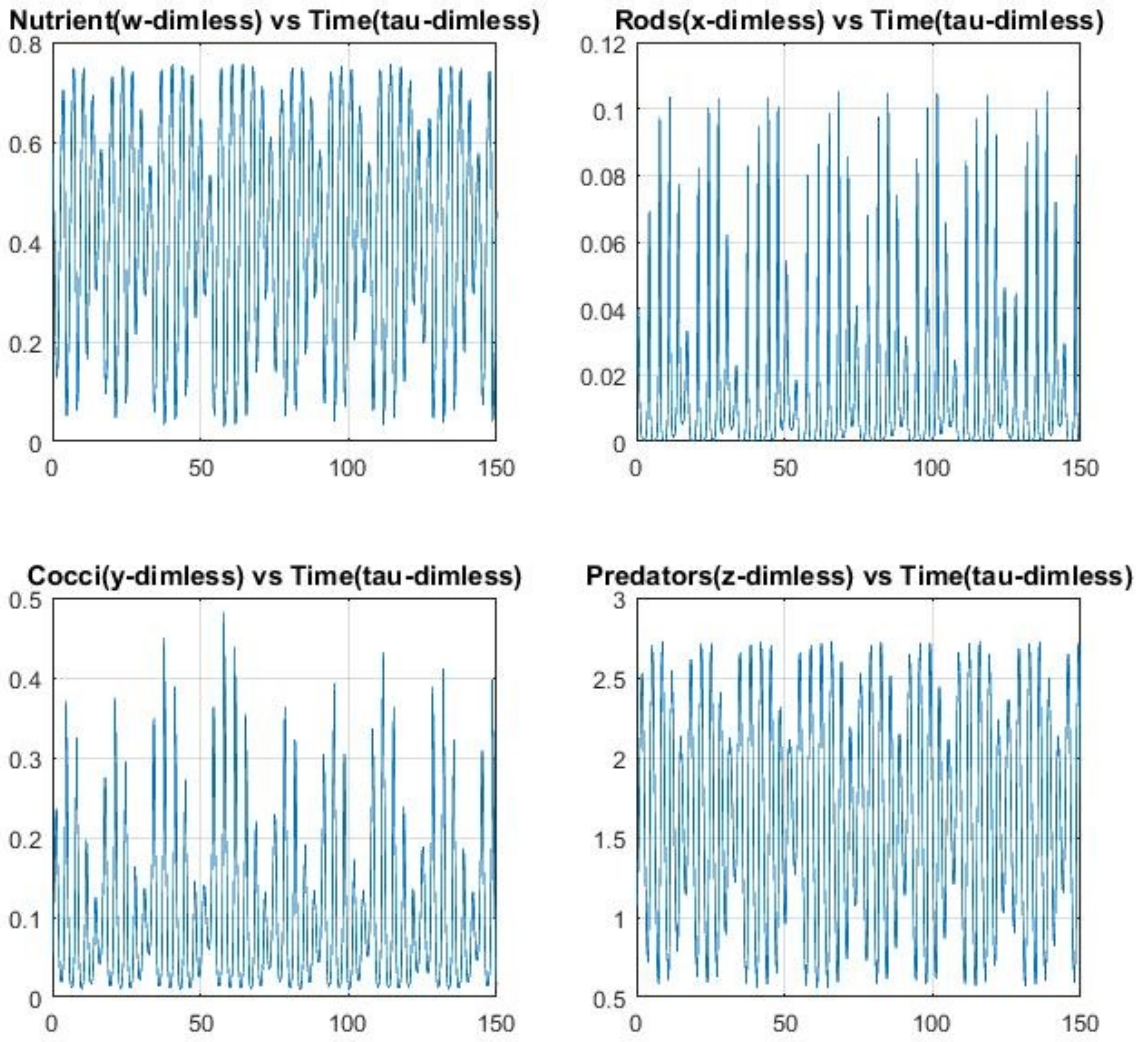

Figure 3.1. Plots of the four dimensionless variables w (nutrient), x (rods), y (cocci) and z (predators). Chaotic dynamics is evident.

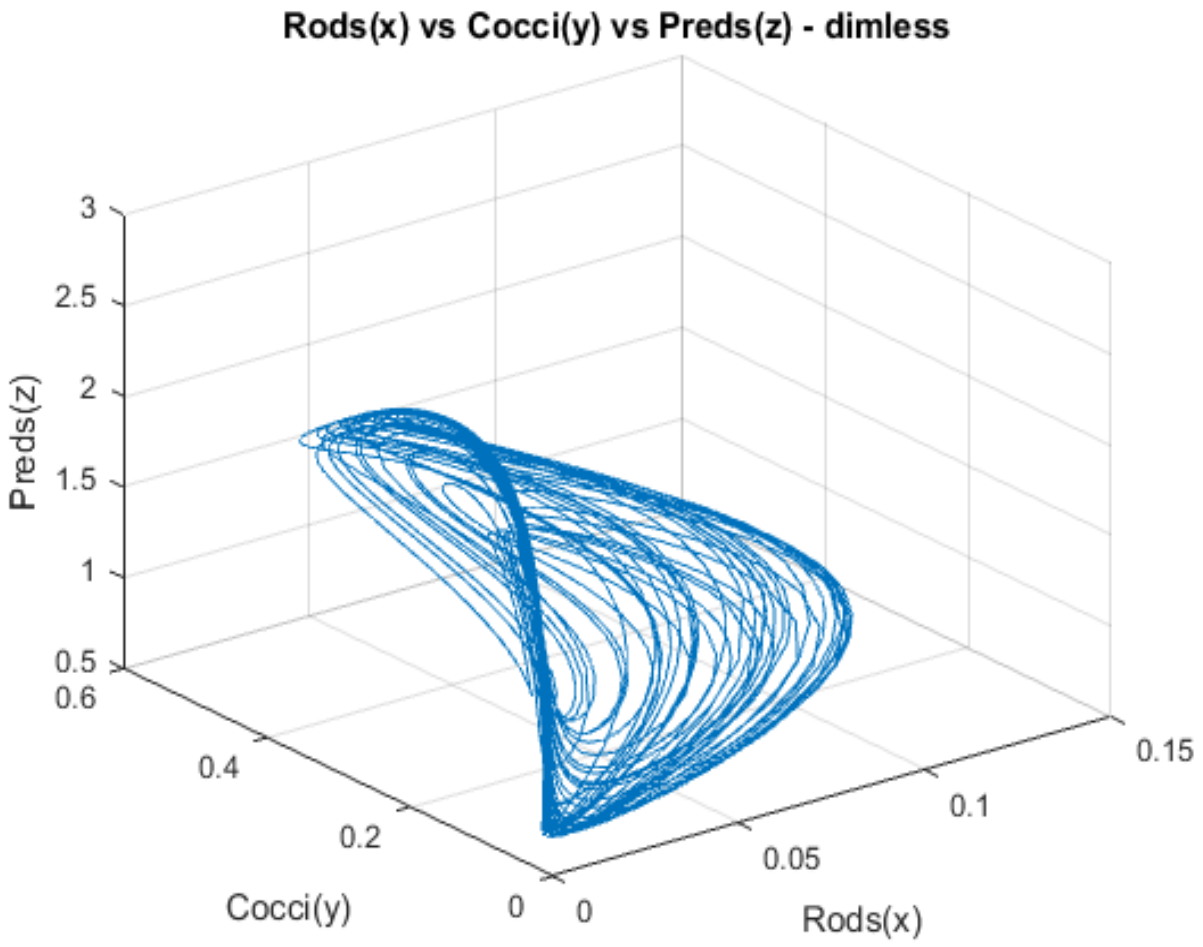

Figure 3.2. A system-space plot of dimensionless rods vs. cocci vs. predators yields the usual 3-D section of the 4-D strange attractor.

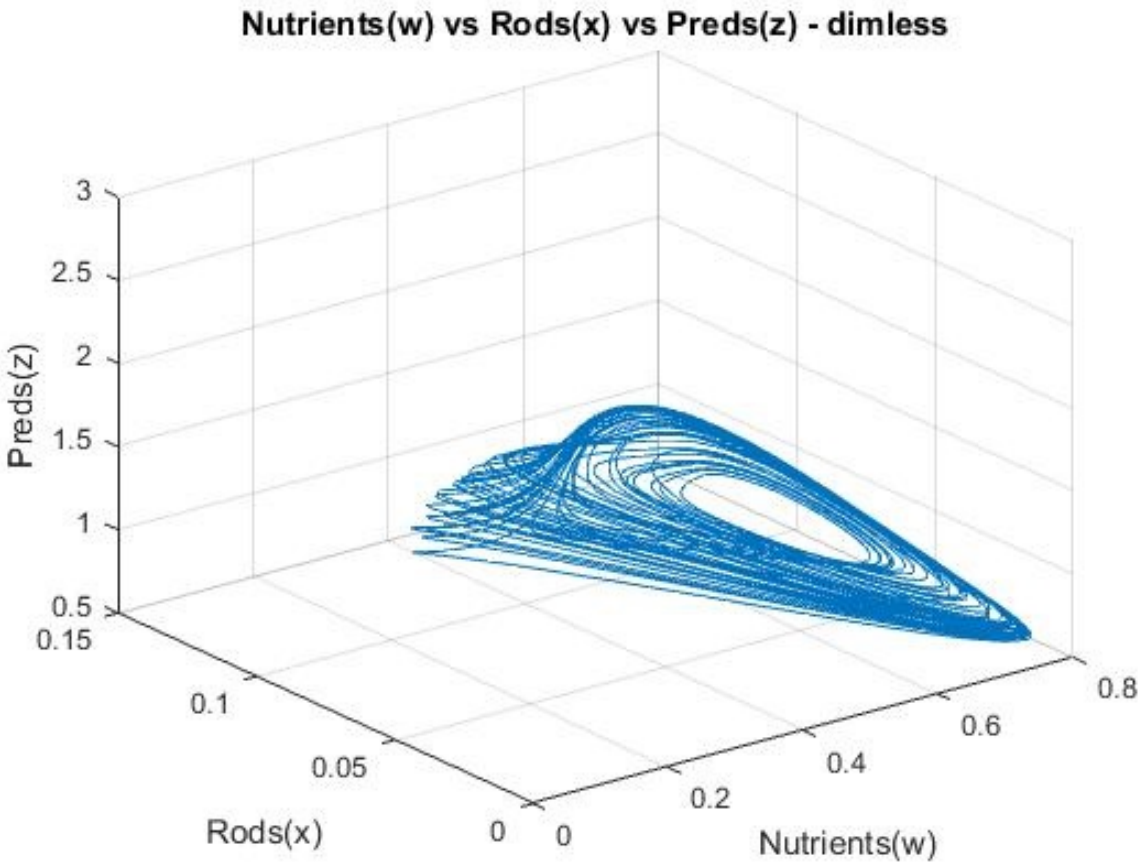

Figure 3.3. Dimensionless system-space 3-D section plot of nutrient vs. rods vs. predators.

It is evident that the appearance of the dimensionless results is essentially the same as the dimensionless cases presented in Chapter 1. Figure 3.1 shows variable plots that are irregular, non-periodic functions of time that are not predictable in detail. This results in a strange attractor plot, 4-dimensional in the general case, that Fraser and Swinney (1986) characterize as having a well-defined, asymptotic probability distribution. Nevertheless, the plots of various variable pairs shown in Figures (3.4) through (3.6) do not show relationships that are random in the classical sense. More recent work by Anishchenko et al. (2004) provides additional

justification for a statistical approach. They divide attractors into the classes of hyperbolic, quasi-hyperbolic and non-hyperbolic. (The well-known Lorenz attractor is of the quasi-hyperbolic type.) They also study the effect of noise on the calculation of invariant measures such as Lyapunov exponents and invariant statistical measures. According to Anishchenko et al. (2004) most chaotic attractors that are dealt with in real experiments and numerical simulations are of the non-hyperbolic type, which is the classification that

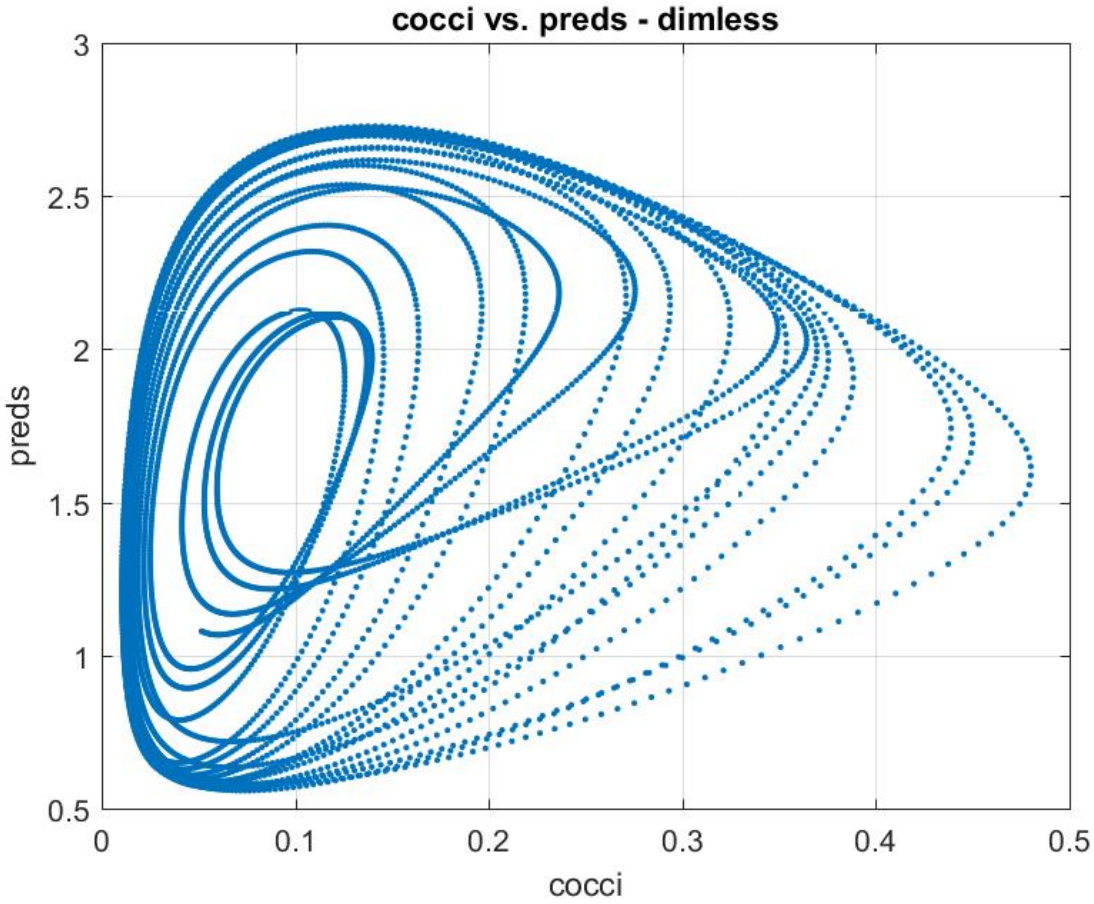

Figure 3.4. Dimensionless plot of predator cells (y-axis) vs. cocci cells (x-axis). Clearly, the relationship is not random in the classical sense.

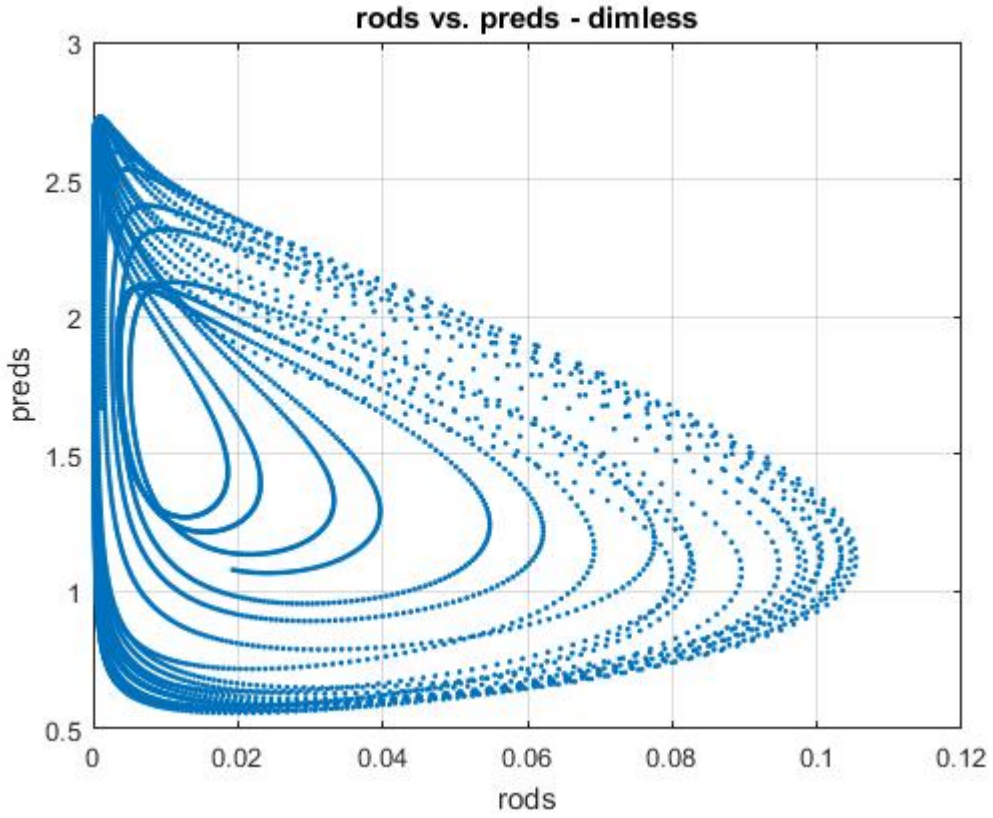

Figure 3.5. Dimensionless plot of predator cells (y-axis) vs. rod cells (x-axis). Again, the relationship is not random in the classical sense.

the attractor in Figure 3.2 probably falls under. Properties of non-hyperbolic attractors are more sensitive to noise, and their statistical properties cannot be proven to exist as rigorously, but they can be approximated by numerical calculation. In Chapter 4 we calculate probability distributions numerically for the variables in Figure 3.1, and the results seem well defined in that stable distributions result as the number of data points are increased. Shannon information concepts and statistics, as they might apply to biological systems, are discussed further in Chapter 4.

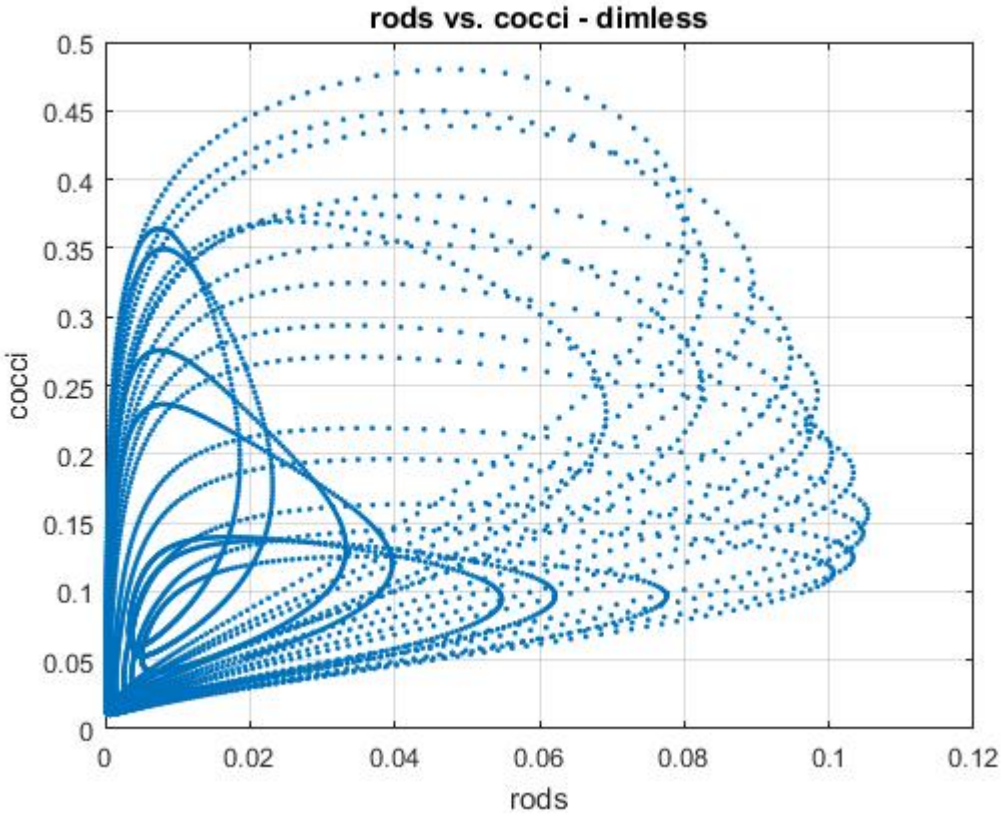

Figure 3.6. Dimensionless plot of Cocci cells (y-axis) vs. rods (x-axis). Again, the relationship is not random in the classical sense

3.5. References.

1. Anishchenko, V., Vadivasova, T., Strelkova, G., and Okrokvertskhov, G. 2004. Statistical properties of dynamical chaos. *Mathematical Biosciences and Engineering 1(1)*: 161-184.
2. Fraser, A. and Swinney, H. 1986. Independent coordinates for strange attractors from mutual information. *Physical Review A 33(2)*: 1134 – 1140.
3. Kot, M., Sayler, G. and Schultz, T. 1992. Complex dynamics in a model microbial system. *Bulletin of Mathematical Biology 54*: 619-648.

Chapter 4: How Might Information Theory Relate to Chaotic Dynamics in Biological Systems?

4.1. Introduction.

If deterministic chaotic dynamics (DCD) can be viewed as some type of sustainable state, then one thing it has in common with classical steady and periodic steady states is that they are time-persistent - meaning that once set up, the states persist indefinitely in a mathematical sense. However, as pointed out by Fraser and Swinney (1986), "Strange attractors are ergodic and have well-defined, asymptotic probability distributions", although as discussed in Chapter 3, the relationship between the variable pairs do not appear random in the classical sense – only non-predictable in detail. (We will return to this later.) Thus, unlike classical steady-states, the attractor variables have Shannon measures of information, something that may make them distinct. Fraser and Swinney (1986) deal with the concept of mutual information because it generalizes readily from discrete probability distributions, mostly studied by Shannon, (Ben-Naim, 2008) to the continuous case. What is commonly called "Shannon information" or "Shannon entropy" does not generalize directly. However, this latter concept is what we will work with initially. Rather than call it information or entropy, for reasons that will become clear, we will call it for now "Shannon's measure of uncertainty"(SMU). For a discrete probability distribution (PD) having n possibilities, Shannon's measure is given by

$$SMU = -\sum_{i=1}^{n} P_i \left(Log_2(P_i) \right) \qquad (4.1)$$

Uncertainty does not sound much like information, so what justifies the uncertainty interpretation?

4.2. Interpretation of Shannon's Measure.

As described in his two clearly written and highly recommended books, Ben-Naim (2008, 2015) describes the puzzling nature of the concept of Shannon Information. He points out that Shannon's original objective was to develop a "measure of information, choice and uncertainty", so as far as Shannon was concerned, one could refer to Shannon's measure of information as Shannon's measure of uncertainty (SMU), with the resulting numbers called bits when base 2 logs are used (natural and base 10 log units are called nats and harts respectively) . Shannon's original motivation was to use the Shannon measure concept and resulting mathematics to manipulate and reproduce digital and other signals (Shannon and Weaver, 1998). As such, it had no relation to the "meaning" contained in the signals, analogous to the task of reproducing a page of words with no concern for what the words mean - just the letters, spaces and their respective probabilities of appearing. In fact, paragraphs conveying identical "meaning" but written in different languages produce different Shannon measures (Ben-Naim, 2015).

If modern information theory is going to find broad application in scientific disciplines, one would expect biological systems to be prime areas of application, because a huge amount of signal and signal processing is involved,

both conscious and unconscious (Bialek, 2012; Eigen, 2013). Within microbes, the continuous signaling process starts with the DNA, and it is combined with "sensory" signals from the surrounding environment. At numerous locations, signals are received, processed and new signals sent out to additional locations. Ultimately, this results in organism behavior, some of which, such as nutrient seeking and threat avoidance, can be observed. Ben-Naim (2008, 2015) makes a clear distinction between what he calls "Shannon's measure of information" and the various types of "meaningful or behavior-inducing information" that he calls "colloquial" information. The obvious question is: how might one relate to the other, because general meaning of some type has to be derived from a Shannon-quantified signal in order for the signal to be of any interest at all, and the "meaning" does not have to be conscious as shown by the Venus flytrap study of Böhm et al. (2016). Can these thoughts be made clearer?

The clarity issue begins immediately when one tries to explain or understand Shannon measure concepts, because all the involved understanding is colloquial. Shannon's measure applies directly to any well-defined discrete probability distribution, and probability distributions are associated intimately with uncertainty, so the uncertainty interpretation is appealing. This is more consistent with the thermodynamic entropy concept that is also viewed by many individuals as a measure of uncertainty. In fact, Ben-Naim (2008) argues convincingly that temperature should have the units of energy, not degrees, making the statistical mechanical interpretation of thermodynamic entropy dimensionless and identical formally to Shannon entropy, although Shannon entropy can apply to probability distributions that have no relation to thermodynamics. So how might the uncertainty

interpretation, Shannons's measure of uncertainty (SMU), be applied to biological systems, and what are the implications?

To begin answering that question, let us consider hunting for food in a forest. Assume there are 20 distinct locations where food might be found, and the task performer (TP) doesn't know where to start. Assume further that the TP has at least a rudimentary consciousness. The best that can be done on the initial search, without some kind of prior knowledge, is to assign a Bayesian probability of 1/20 to each location and start looking. This would be equivalent to maximizing the SMU (maximum uncertainty principle) to arrive at the "best" initial estimate of the underlying PDF (Jaynes, 1957; Ben-Naim, 2015). When the food is found, the TP knows where it was, and the first trial uncertainty (sometimes called missing information) is removed - which could be at the first location observed, the final location or any location in between. If the food location is and will always be truly uniformly random, the TP can never do better than random guessing (maximum uncertainty), and Shannon's Measure takes on its maximum possible value for that particular task given by:

$$SMU_{\max} = -\sum_{i=1}^{20} P_i Log_2(P_i) = +20[\frac{1}{20} Log_2(20)] = 4.32 \ \ bits, \qquad (4.2)$$

This result is consistent logically with viewing the SMU as a measure of uncertainty or degree of randomness, and Grassberger (1991) alludes to this by suggesting that the phrase "net flow of (Shannon) information" would be better expressed as "net flow of Shannon ignorance". Still another viewpoint would be that the combined system including the TP would always stay at maximum Shannon entropy.

Let us now suppose that the food location is not truly random, but follows a discrete, objective probability distribution, with P_i being equal to 0.01 at each location except location 7 where it is 0.81. Now it is possible, with repeated food searches, to discover that food will be found at location 7 about 80% of the time, and this knowledge we view as the potential development of colloquial information and a decrease in the SMU. This more refined (less random) probability distribution has a Shannon measure of

$$SMU = -\sum_{i=1}^{20} P_i Log_2(P_i) = -19\left[0.01 Log_2(\frac{1}{0.01})\right] + 0.81 Log_2\left[\frac{1}{0.81}\right] = 1.51\, bits, \qquad (4.3)$$

The SMU decreases as the probability distribution becomes less random, and the ability to find food on the 1st try, and on average over many tries, increases. So for a given task, if the SMU is low compared to its maximum possible value ($Log_2(n)$), the task becomes easier to accomplish with repeated trials. Thus, we see the development of colloquial information as a time-dependent process resulting from an improved understanding of the PD underlying the SMU with repeated task performance.

This discussion is implying that a particular SMU value is the result of an interaction between a PD and a particular task performer. In a more abstract sense, this may be what Grassberger (1991) meant by the statement, "---- complexity will be viewed as a property not exclusively associated with the observed object, but rather as a subjective property reflecting the observer-object relationship." In order to calculate a SMU, a set of events and their respective probabilities are needed, but where does this sense of probability come from if not from the knowledge of an observer or task performer? In natural systems such knowledge can be highly indirect, involving various conditional probabilities. As the TP improves based on the use of prior

information from previous search attempts, the process takes on a subjective, Bayesian nature (Gillies, 2000; Bernardo and Smith, 2001).

If a TP has conscious memory of some type, then one can see how a rudimentary understanding of a probability distribution associated with a SMU can be developed and refined, but what about the unconscious case? Evolution by mutation and natural selection appears to be unconscious, but there is a "memory" of successful past mutations retained in the genes (DNA) of a species. As an example of the end (present time) result of probability refinement on an evolutionary timescale associated with a task, let's consider in more detail the insect capture and digestion methodology of the Venus flytrap, mentioned previously and elucidated in biochemical detail by Böhm, et al. (2016). The Venus flytrap has a leaf that closes, potentially trapping an insect, when its hair cells are stimulated. Obviously, it is important to close and begin the digestive process only when an insect is present, not just an inanimate particle of some type blown in by the wind, wind turbulence alone or the touch of a nearby plant. What started the flytrap species down the insect-capturing pathway initially is unknown; in fact, one can imagine multiple possibilities for starting points. So what is the probability that "hair cell stimulation" means "insect present"? Obviously, if the probability was overestimated, the plant would be wasting a lot of its metabolic energy capturing and tying to digest junk. Here's how the plant got sufficiently close to the true probability that "stimulation implies insect". A) One hair cell stimulation and nothing more → ignore; B) a 2nd stimulation within about 20 sec. of the 1st → close and wait; if nothing more, reopen; C) 1st additional stimulation after closing → start the digestive process; D) 3rd stimulation after closing → proceed with digestion and activate full nutrient uptake. The big

difference between inanimate hair-cell stimulations and insects, is that the insect craws and wiggles when confined, so presumably through the process of mutation and natural selection the flytrap species has acquired a methodology to time and count the possible insect stimulations. If a set of stimulations is within an acceptable pattern, then the probability of an insect being present is sufficiently high that on average, leaf closing, digesting and nutrient absorption is energetically positive for the plant. If the net energy expenditure could not be made positive, then presumably the insect consuming methodology would not have evolved. The essential process seems to be trial and error (mutations) along with preserving DNA mutations (memory) that increase plant survival on average (natural selection). Evidently, consciousness is not required, but DNA entities interacting with the natural world can form at least rudimentary memories of a probabilistic nature.

4.3. The concept of Redundancy.

So far we have focused on the uncertainty interpretation of Shannon's measure, so why is Shannon's development commonly called "information theory"? This is clarified by realizing that knowledge and uncertainty are the opposite of each other when dealing with PD structure. When characterizing a PD, decreasing SMU means increasing information about PD structure and vice-versa. This inverse relationship between uncertainty and information is what makes Shannon's measure so confusing when calling it some type of "information", and as pointed out by Ben-Naim (2008, 2015), there is an immense amount of confusion in the public literature. This inverse

relationship can be clarified further by employing a normalized measure to characterize the degree of non-randomness in a probability distribution defining a SMU called the redundancy R. It is defined by (Ben-Naim, 2015):

$$R = \frac{\left(SMU_{\max} - SMU\right)}{SMU_{\max}}. \tag{4.4}$$

So R can be used to distinguish between a totally random process within a specified domain (SMU = SMU_{max} → R = 0) and an event with a probability of one (SMU = 0 → R = 1). Thus, for the probability distribution associated with Equation (1) R = 0, and for Equation (2):

$$R = \frac{\left(4.32 - 1.51\right)}{4.32} = 0.65 \tag{4.5}$$

Evidently, R is a measure of how much information can be obtained about the nature of a probability distribution through repeated sampling. One can imagine that the degree of sophistication of this mental process can vary widely. For example, many small prey animals, such as rodents, are more active at particular times during the day, such as early morning or late afternoon. By merely recognizing and retaining this in some way, a predator could choose to be especially active during such time periods in particular locations, and thereby increase the probability of hunting success. At the other extreme we have humans, who often spend a lifetime, or multiple lifetimes (culture), trying to improve success on a particular task.

An interesting question related to probability that arises with humans is the possible relationship between evolving subjective probability and the underlying objective probability if the latter actually exists. Consider the gambling industry and the game of roulette with a perfect roulette wheel (Although no roulette wheel is perfect.). For each possible bet, an objective

probability can be calculated, and for any bet the player on average will lose. A true beginning player will have no knowledge of the relative probabilities of the different bets (internal SMU = SMU_{max}), but through study and practice perhaps the actual probabilities could be learned and remembered by the player, so that the internal SMU and the objective SMU would be closer to the same. Such a player still could not win on average, but he/she could do better on average than an inexperienced player. The experienced player would be taking advantage of the learnable redundancy in the objective probability distribution. In the extreme, it would appear that learning can sometimes reduce a subjective probability distribution to a redundancy of 1 (SMU of 0), leading to the realization that the process studied is actually deterministic, perhaps in a complex way, not random. The main process for doing this has been the "scientific method". New ideas are analogous to mutations, and successful experiments are analogous to natural selection.

The concept of redundancy as a measure of degree of non-randomness appears fundamental and essential to the origin and evolution of living systems (Wagner, 2014). What if one asked the question: "Assuming that at least one amino acid combination will be successful, what is the probability that a random enzyme composed of 347 amino acids, like the ADH1 protein in Yeast (Raj et al., 2014), will enable the fermentation of glucose to ethanol?" Superficially, the question seems reasonable in an experimental sense. One would simply begin by building each combination and checking its catalytic capabilities. The number of successes divided by the total number of unique combinations would be the desired probability. If one assumed a redundancy of zero in the applicable probability distribution, then each 347-member combination would be equally probable and the SMU would be maximum. So

how many combinations would one have to check? Since there are about 20 amino acids that appear in natural proteins, the unbelievable number is 20^{347} possible combinations - much, much larger than the total number of hydrogen atoms in the entire universe (about 10^{90}, Wagner (2014)). Only if there were a redundancy near one in the applicable probability distribution, could the Yeast species have found a successful enzyme through mutation and natural selection during the time that Earth has existed (about 5 billion years or only 10^{17} seconds!). As presented in the seminal work summarized by Wagner (2014), such redundancy is absolutely essential to Darwin's theory of evolution by mutation and natural selection, and this fact has been largely hidden in the structures of life, only now starting to be realized.

Another interesting implication of information theory is that the willingness to gamble, consciously or unconsciously, is essential to the development of life. When one faces a new task with a desired outcome, such as finding food without being injured or killed, one adopts the best plan available and proceeds with the task. This is the essence of gambling. Then one follows the dictum: "If once you fail, try, try again". As one's understanding of the PD involved increases, the probability of success also increases. In the human case, perhaps some mix-up in processing all of this is behind the phenomenon called "pathological gambling' where the involved PD is structured by other humans so that the probability of success is always less than 1/2 no matter how many times the task is repeated. But we all have to gamble a little in order to be successful in life.

4.4. What About Continuous Probability Densities?

When dealing with discrete PDs having uniform probability P = 1/n, the maximum SMU is always given by:

$$SMU_{\max} = -\sum_{i=1}^{n} \frac{1}{n}\left(Log_2(\frac{1}{n}) \right) = \frac{n}{n} Log_2(n) = Log_2(n) \,, \qquad (4.5)$$

and one can observe that SMU_{max} goes to infinity as n goes to infinity. This makes sense, because if one has an infinite number of choices of equal probability, then one has infinite uncertainty.

Transformation to the continuous case is presented in Appendix I of Ben-Naim (2008), and we will outline his procedure below. Let us assume that there is a probability distribution for the rod population, r(t), shown in Figure 1.3. Let the resulting probability density function be given by, PF_r, defined on its respective interval, with the associated random variable being R. Then using PFr defined on interval (a,b) we want:

$$Pb(r_1 \le \mathrm{R} \le \mathrm{r}_2) = \int_{r_1}^{r_2} PF_r(r)dr, \;\; with \;\; \int_{a}^{b} PF_r(r)dr = 1 \qquad (4.6)$$

Now divide the interval (a,b) into n parts of equal width w=(b – a)/n, with r_1 = a,

r_i = a + (i-1)w and r_{n+1} = a + nw = b. Then for any interval bounded by r_i and r_{i+1} , the probability, P, of falling in that interval, as it depends on i and n, is:

$$P(i,n) = \int_{r_i}^{r_{i+1}} PF_r(r)dr \qquad (4.7)$$

Then for some finite n, the Shannon Measure, now called $SM_r(n)$, is given by:

$SM_r(n) = -\sum_{i=1}^{n} P(i,n)Log_2[P(i,n)]$, which is equivalent to:

$$SM_r(n) = -\sum_{i=1}^{n} \left[\int_{r_i}^{r_{i+1}} PF_r(r)dr\right] Log_2 \left[\int_{r_i}^{r_{i+1}} PF_r(r)dr\right] \qquad (4.8)$$

With several additional steps, Ben-Naim (2008) shows that as $n \to \infty$, Equation (4.8) becomes:

$$SM_r = -\int_a^b PF_r(r)Log_2[PF_r(r)]dr - \lim_{n \to \infty} Log_2\left(\frac{b-a}{n}\right), \qquad (4.9)$$

which obviously goes to infinity as n approaches infinity, but the integral portion is finite. We also note that probability density values, unlike true probability, can be greater than one, which can lead to negative SM values, something that never happens with true probabilities which are always < 1.

The Integral portion of Equation (4.9) appears well-defined mathematically, but what it now means physically is not clear. It is certainly different from the discrete case, which is always maximized by the uniform,

discrete distribution, so the concept of redundancy is also not defined immediately. Accordingly, this potential line of development will not be followed further in this chapter.

4.5. Calculation of Chaotic Information Measures.

In earlier portions of this chapter, we discussed learning about the nature of discrete probability distributions in natural systems as being a Bayesian (subjective) process, and the concept of a continuous probability density function is highly abstract (Think of the fly trap example). In addition, virtually all living systems are not concerned about tiny differences in the measures of variables that vary over large ranges. One part in 10 might be of interest, but not one part in 100 or 1000. So in calculating information measures for chaotic distributions we will continue to use discrete approximations to the variable distributions. In addition, Shannon's measure of uncertainty is dimensionless, along with redundancy, so we will work with the dimensionless forms of the coupled nonlinear system that was developed in Chapter 3.

Calculating numerically a trajectory along a strange attractor appears equivalent to a sampling process, in that the round-off error at each time step will alter the following calculations. This invites one to calculate a discrete probability distribution for each of the chaotic time series that results (See Figure 3.1), and a set of distributions are shown in Figures 4.1 through 4.4. The figures are arranged from the lowest to the highest redundancy values, which along with the Shannon measures are given in Table 4.1.

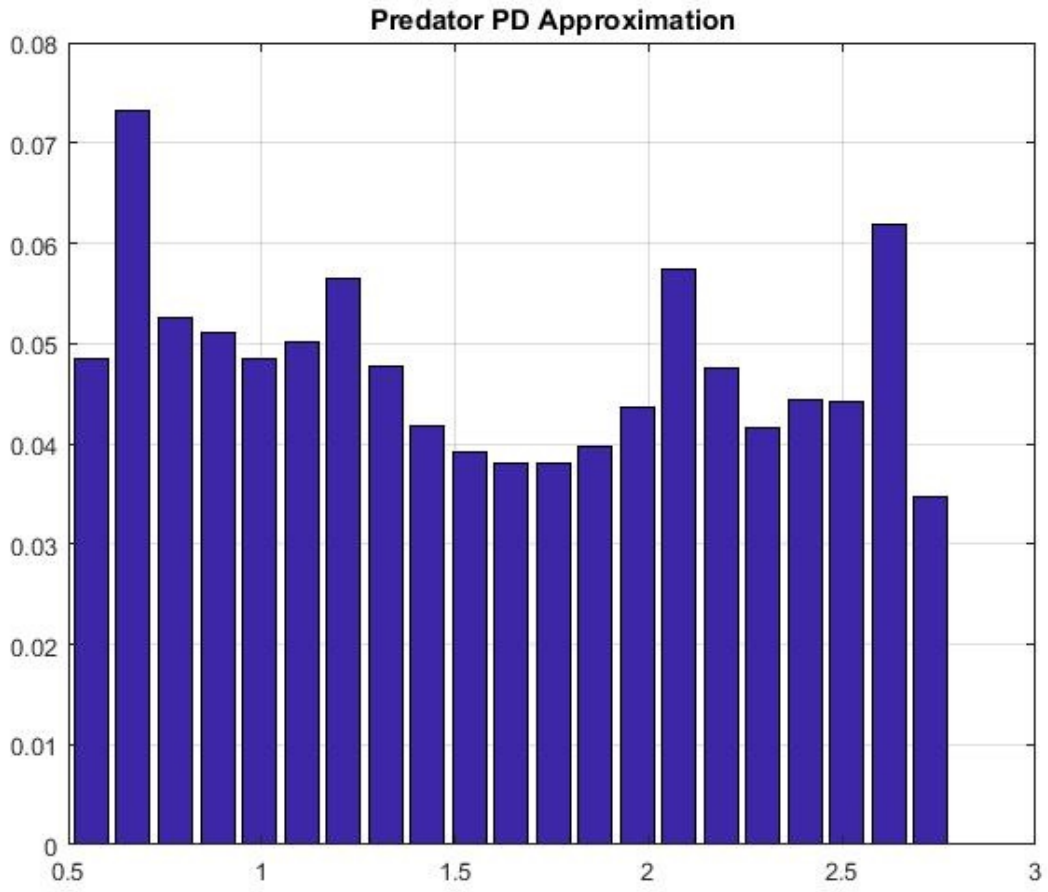

Figure 4.1. Discrete probability distribution for the dimensionless predator values shown in Figure 3.1. The domain of values was divided into 21 ranges of equal width 1.085E-1.

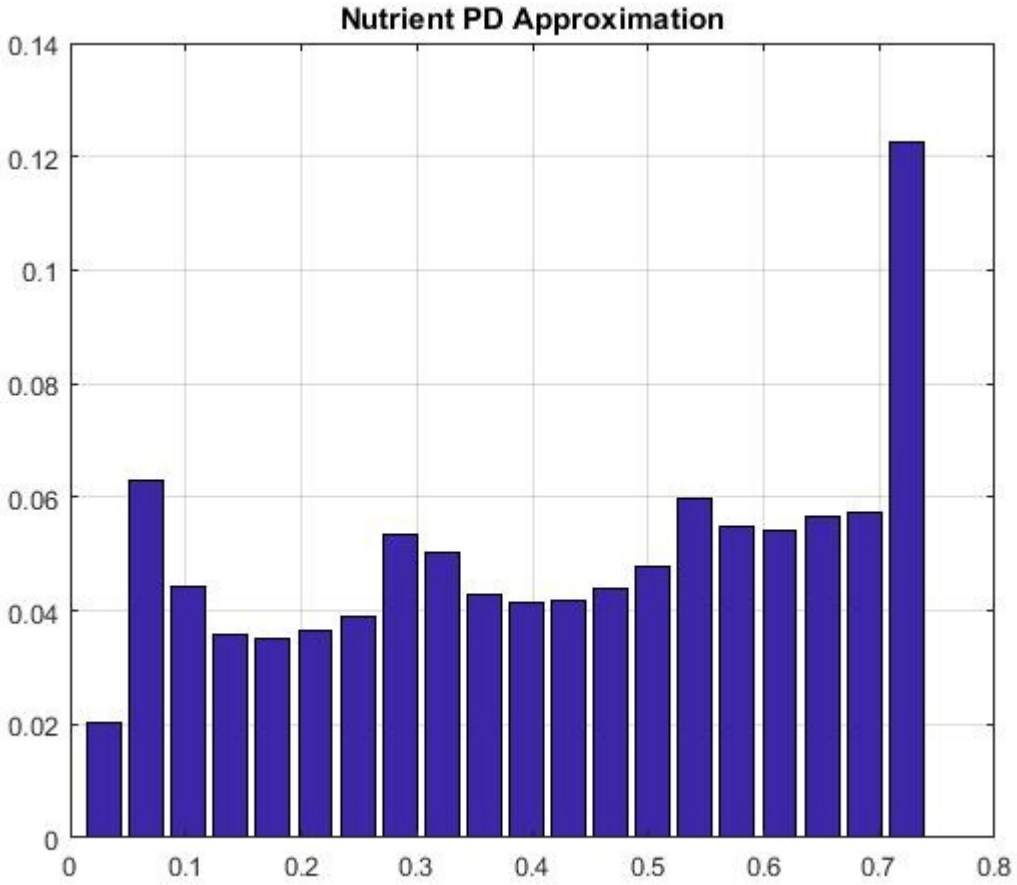

Figure 4.2. Discrete probability distribution for the dimensionless nutrient values shown in Figure 3.1. The domain of values was divided into 21 ranges of equal width 3.6525E-2.

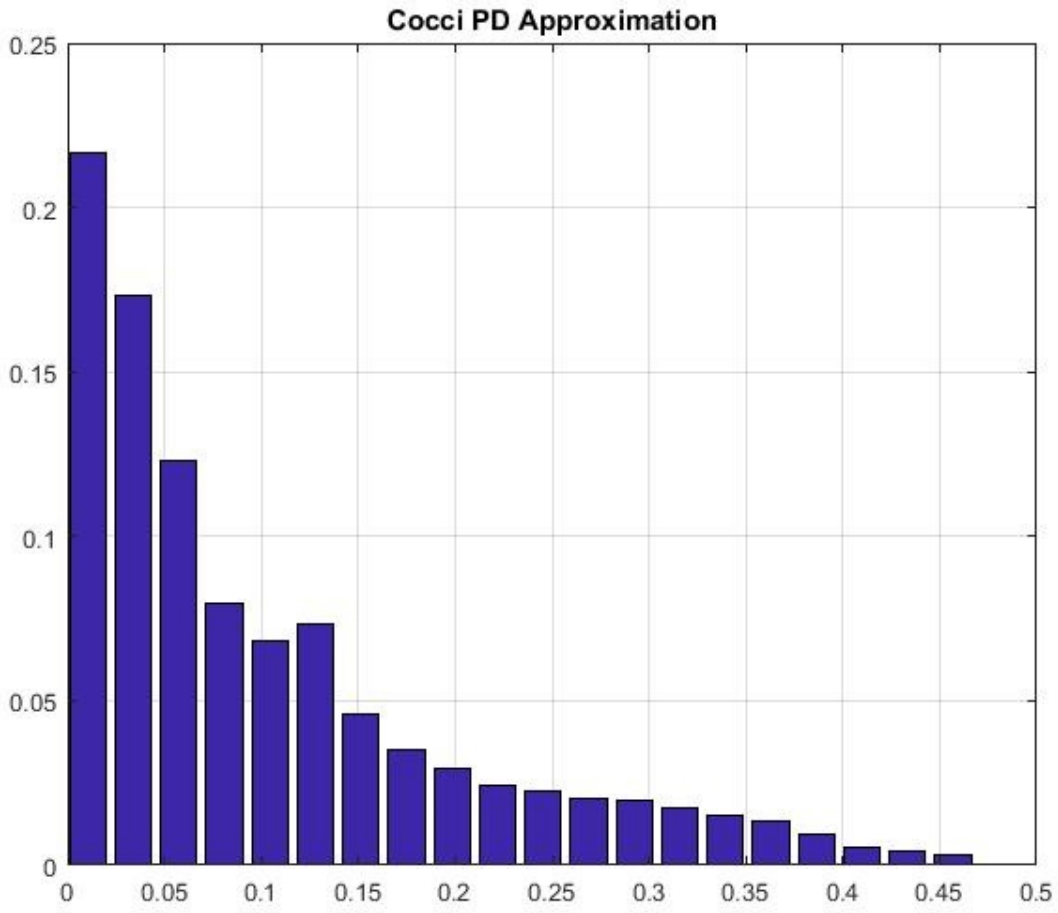

Figure 4.3. Discrete probability distribution for the dimensionless cocci values shown in Figure 3.1. The domain of values was divided into 21 ranges of equal width 2.35E-2.

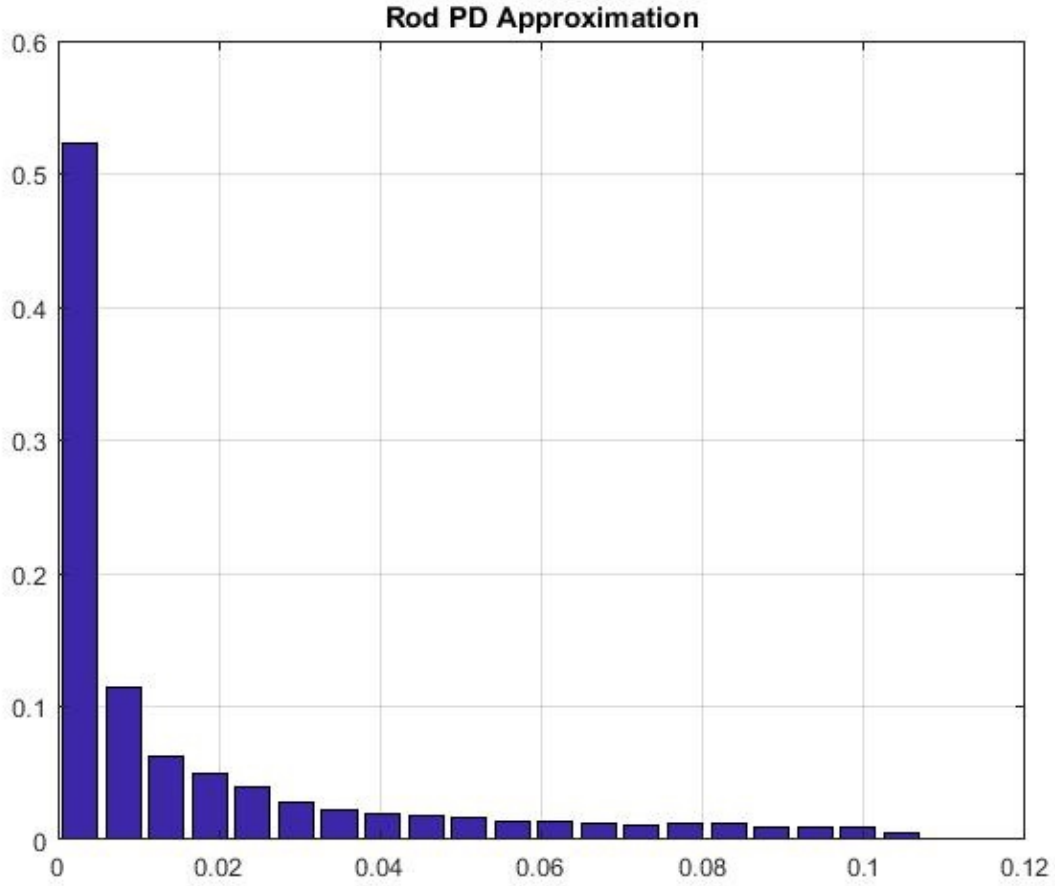

Figure 4.4. Discrete probability distribution for the dimensionless rod values shown in Figure 3.1. The domain of values was divided into 21 ranges of equal width 5.3625E-3.

Table 4.1. Values for Shannon's measures of uncertainty (SMU) and the resulting redundancy (RD) values for the discrete probability distributions shown in Figures 4.1 through 4.4. The maximum possible SMU = $(29)^{1/2}$ = 4.392.

Concentrations	Shannon's Measure	Redundancy
Predators	4.368	0.005464
Nutrients	4.235	0.0366
Cocci	3.566	0.1881
Rods	2.771	0.369

Looking at the four figures and the corresponding SMU and RD values in Table 4.1, we see that as the PDs become more structured (less uniformly random), the SMU values decrease and the RD values increase. In this situation, the predators apparently have the best deal. Their concentrations, stay well above zero, and they are not highly erratic. The cocci have the 2nd best deal and the rods come in last. Both nutrient-consuming microbes, however, have high probabilities of being at the low end of their concentration ranges where survival is the most precarious. The nutrient concentrations do not appear to be especially limiting, with a probability trending toward the high concentration end. It would appear that the rods and to a lesser extent the cocci are fighting for survival, but as long as the system stays on its chaotic attractor it is sustainable. The predators change their consumption emphasis between rods and cocci so that they are relatively well fed without destroying one of their food sources.

4.6. Summary and Future Research Suggestions.

Due to the common observation of extreme sensitivity of mathematical models of ecological/microbial systems producing DCD to parameter variations, we have suggested that something fundamental may be missing from the current mathematical formulations. Unlike the classical steady or periodic steady states, a strange attractor has several Shannon measures including SMU and R. So how might one begin to incorporate such concepts into the modeling process?

We can't answer this question fully, but to begin the process a logically and mathematically consistent interpretation of Shannon Information Theory as applied to ecological systems is presented. In such a development, what is commonly called Shannon's measure of information is identified as a measure of uncertainty relative to the structure of the involved discrete probability distribution, with maximum uncertainty occurring when the PD is uniform. As the relevant PD takes on more structure, the SMU decreases as Bayesian (colloquial) information concerning the structure increases. The PD property called redundancy is presented as a convenient dimensionless measure of uncertainty, taking on the value of zero when the involved PD is uniform (maximum uncertainty) and the value of unity when the PD has one unique value and actually represents a deterministic process (no uncertainty).

It its original application to digital and other types of communication, it is easy to confuse the colloquial or common information that a message may contain, and be read by a human observer (decoder), and the actual Shannon information that relates to the probability and structure of the various symbols that compose the message – nothing more. In the ecological/microbial application this problem is removed by identifying

colloquial information with the (Bayesian) knowledge that a task performer may develop as her/his colloquial knowledge of a PD increases with repeated task performance. As a task subject to a certain PD is repeated, the task performer can develop prior and improving understanding of PD structure, and this subjective Shannon measure of uncertainty will decrease or the PD redundancy will increase. If the actual PD structure is truly uniform and random, a task performer can never learn from repeated task performance and the SMU will stay at its maximum value with a zero redundancy.

As an elementary application of these concepts, we calculated the Shannon measure of uncertainty and the related redundancy for each member of a four-component chemostat involving a nutrient and three microbes. The actual experiment demonstrated DCD (Becks et al., 2005), but the calculations were based on the output of a recently published model that also produced DCD for a certain parameter set (Faybishenko et al., 2018). Of the three microbes involved, a rod, coccus and ciliate predator, the predator held the most dominant position and the rods the least dominant position. The result was a redundancy of 0.005 for the predator's PD, 0.188 for the cocci PD and 0.369 for the rod's PD. Thus, in a PD sense the predators had the least structured PD, while the rods had the most structured. The overall objective of the rods and cocci was to compete for the available nutrients, while the objective of the predator was to consume rods and cocci without wiping out either microbe class. Presumably, each microbe would attempt to optimize its individual situation in the continuously changing chemostat environment. How this might be done is not clear and probably not incorporated into the model in a complete way.

It is worth devoting more discussion to the sense in which the chemostat variables (n, r, c, p) can be represented by the PDs shown in Figures 4.1 through 4.4. The references dealing with this question in the most mathematically rigorous manner are Fraser and Swinney (1986) and Anishchenko et al. (2004). Both references conclude that strange attractors are typically ergodic, with well-defined asymptotic probability distributions, although this can be proven more rigorously for some attractor classes than others. At the same time, Figures 3.4 through 3.6 show that when various variables are plotted against each other, the result does not appear random in the classical sense; the plots appear more deterministic. Due to extreme sensitivity to initial conditions (Lyapunov exponent > 0), a numerical solution producing DCD is equivalent to an ultimately unbiased sampling of the phase space if the initial trajectory points influenced by the particular starting point are thrown out (Fraser and Swinney, 1986). The solution round-off error at each numerical step (not just the first) influences future values in such a way that mathematical predictably is lost, so the result becomes a sampling of an ergodic (independent of attractor starting point) distribution of points. Such a sampling has a mean, variance and additional statistical measures – a class of numbers that are structured, bounded, but unpredictable in a deterministic sense.

The mathematics of information theory goes well beyond the simple calculations presented in this chapter. As described in Kantz and Schreiber (2004), several other Shannon information-motivated measures have been developed for analyzing random or chaotic time series not necessarily applied to microbial population dynamics. The concept of mutual information has found several applications (Fraser and Swinney, 1986). In dealing with

microbial population dynamics, however, it appeared initially that the so-called "transfer entropy" of Schreiber (2000) might be particularly useful. As stated in his abstract: "The standard time-delayed mutual information fails to distinguish information that is actually *exchanged* (between time series members) from shared information due to common history and input signals. The resulting transfer entropy is able to distinguish effectively driving and responding elements and to detect asymmetry in the interaction subsystems." These appear to be very promising concepts when applied to microbial and other types of ecological systems.

However, James et al. (2016) maintain that transfer entropy cannot be viewed as an information flow. According to Cructhfield (2018, Personal communication.), another promising candidate for information transfer is the cumulative residual entropy of Rao et al. (2004). This measure also has the potential advantage of being applicable to probability density functions as well as discrete distributions. The potential relation of chaotic dynamics to the appropriate information flows, being careful of what "information" actually means in an ecological context, appears very interesting, and it should be considered as a prime area for future research. The discussion involving a task performer was dynamic, but the Shannon measures based on a strange attractor appear to be some type of average. Thus, there is a clear need to bring in system dynamics

Another question is, how does one build a precise mathematical model of the interacting components (task performers) of an ecological system that reproduces the DCD observed in an experiment or possibly in the natural environment? In considering the Becks et al. (2005) experiment, the microbes involved respond to their changing environment in a continuous manner. The

responses are directed by meaningful (colloquial) information obtained from their individual genetic codes and related metabolism. Here we must be very careful. What is commonly called the Shannon measure of information (that we have called SMU) applied to the genetic code, has no relationship to the meaning carried by or derived from decoding. The meaning is derived by the decoding process involving an energy source, ribosomal synthesis of proteins, and the resulting metabolic processes. The associated microbial responses would be expected to have extensive flexibility and variability in responding to the changing environment, derived from millions of years of evolution. This leads us to question whether a precise mathematical model reproducing the coupled dynamics would contain any parameters that would be constants. If all parameters are functions of the dependent variables, how can they be measured in detail for highly variable systems prior to the actual experiment? Such an unsolved problem could also be a source of instability in a mathematical model producing DCD that was observed in an experiment.

4.7. References.

1. Becks, L., Hilker, F., Malchow, H., Jürgens, K. and Arndt, H. 2005. Experimental demonstration of chaos in a microbial food web. *Nature Letters 435*: doi:10.1038/nature03627.
2. Ben-Naim, A. 2008. *A Farewell to Entropy: Statistical Thermodynamics Based on Information*. World Scientific, London, UK.
3. Ben-Naim, A. 2015. *Information, Entropy, Life and the Universe*. World Scientific, London, UK .

4. Bernado, J. and Smith, F. 2001. Bayesian theory – book review. *Measurement Science and Technology 12*: 221.
5. Bialek, W. 2012. *Biophysics, Searching for Principles*. Princeton University Press, Princeton, NJ and Oxford, UK.
6. Böhm, J., et al. 2016. The Venus flytrap *Dionaea muscipula* counts prey-induced action potentials to induce sodium uptake. *Current Biology 26*, 286-295.
7. Eigen, M. 2013. *From Strange Simplicity to Complex Familiarity: A Treatise on Matter, Information, Life and Thought*. Oxford University press, Oxford, UK.
8. Fraser, A. and Swinney, H. 1986. Independent coordinates for strange attractors from mutual information. *Physical Review A 33(2),* 1134 – 1140.
9. Gillies, D. 2000. *Philosophical Theories of probability*. Routledge, London and New York.
10. Grassberger, P. 1991. Information and complexity measures in dynamical systems. In, Atmanspacher and Scheingraber, *eds. Information Dynamics*, Plenum Press, New York.
11. Jaynes, E. 1957. Information theory and statistical mechanics. *Physical Review 106*, 620.
12. Kantz, H. and Schreiber, T. 2004. *Nonlinear Time Series Analysis*. 2nd ed., Cambridge University Press.
13. Raj, S., Ramaswamy, S. and Plapp, B. 2014. Yeast alcohol dehydrogenase structure and catalysis. *Biochemistry 53*: 5791-5803.
14. Schreiber, T. 2000. Measuring information transfer. *Physical Review Letters 85*: 461-464.

15. Shannon, C., and Weaver, W. 1998. *The Mathematical Theory of Communication.* University of Illinois press, Urbana, IL.

16. Wagner, A. 2014. *Arrival of the Fittest*. CURRENT, Penguin Group, New York, NY.